AD-A067 233 AERONAUTICAL RESEARCH LABS MELBOURNE (AUSTRALIA) F/G 20/4
A SIMPLE METHOD OF ADAPTING A WIND TUNNEL SCHLIEREN SYSTEM FOR --ETC(U)
JUN 78 N POLLOCK

UNCLASSIFIED ARL/AERO NOTE-378 NL

| OF |
AD A067233

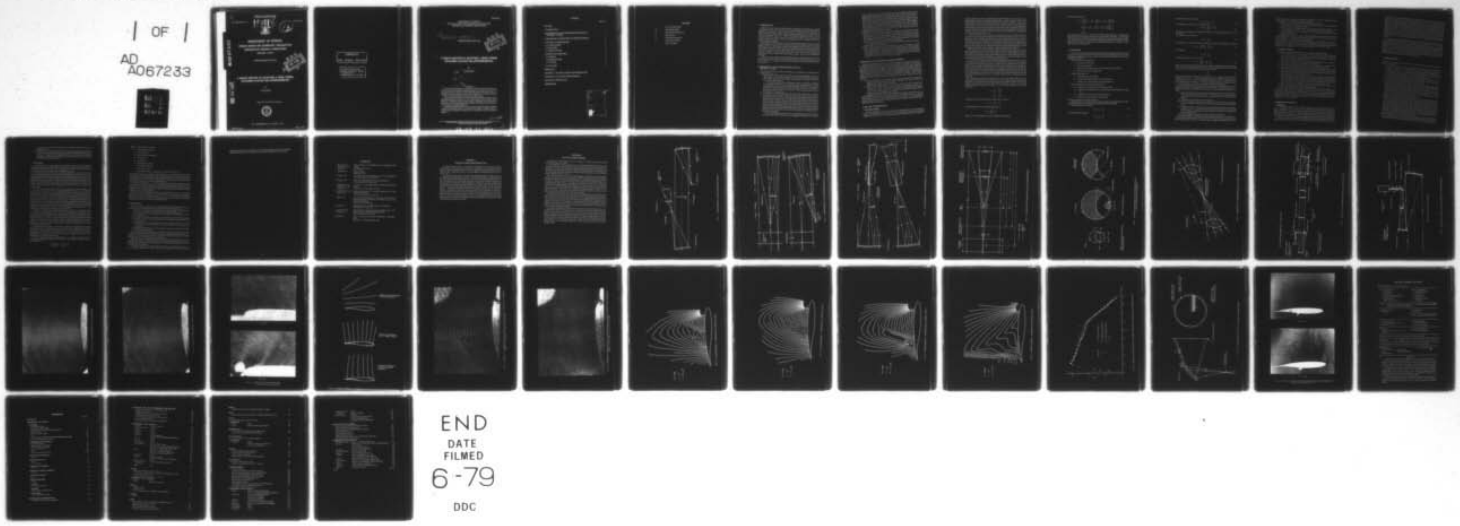

END
DATE FILMED
6-79
DDC

UNCLASSIFIED

ARL-AERO-NOTE-378

AR-001-281

DEPARTMENT OF DEFENCE

DEFENCE SCIENCE AND TECHNOLOGY ORGANISATION

AERONAUTICAL RESEARCH LABORATORIES

MELBOURNE, VICTORIA

AERODYNAMICS NOTE 378

A SIMPLE METHOD OF ADAPTING A WIND TUNNEL SCHLIEREN SYSTEM FOR INTERFEROMETRY

by

N. POLLOCK

Approved for Public Release.

COPY No 15

JUNE, 1978

AR-001-281

DEPARTMENT OF DEFENCE
DEFENCE SCIENCE AND TECHNOLOGY ORGANISATION
AERONAUTICAL RESEARCH LABORATORIES

(17) ARL/AERO NOTE-378

AERODYNAMICS NOTE 378

(6) # A SIMPLE METHOD OF ADAPTING A WIND TUNNEL SCHLIEREN SYSTEM FOR INTERFEROMETRY

by

(10) N. POLLOCK

(11) Jun 78

(12) 43p.

SUMMARY

A simple method of adapting a wind tunnel Schlieren system for interferometry is described. This new interferometer arrangement employs a laser light source, a lens which splits off the reference beam after test beam expansion and a lens and Lloyd mirror to recombine the two beams. The reference beam passes through the test section but is contracted to a narrow waist and displaced well away from the model location.

The proposed design combines a number of favourable characteristics which render it particularly useful for wind tunnel tests. These characteristics include: simplicity, optical robustness, low vibration sensitivity, modest coherence requirements and ease of interferogram analysis. The main disadvantage is that slightly less than half of the total field of view can be recorded on a single interferogram.

Interferograms obtained from tests on a prototype instrument based on a Schlieren system of low mechanical rigidity are presented. Also included is a comparison between aerofoil pressure distributions obtained by direct measurement and by interferogram analysis.

008650

POSTAL ADDRESS: Chief Superintendent, Aeronautical Research Laboratories,
Box 4331, P.O., Melbourne, Victoria, 3001, Australia.

CONTENTS

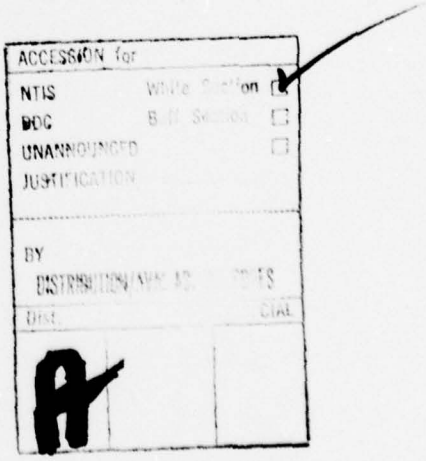

NOTATION

c	Chord of aerofoil model
M	Tunnel Mach number
R	Reynolds number (based on c)
P	Static pressure
H	Free stream total pressure
x	Chrodwise co-ordinate
α	Angle of incidence

1. INTRODUCTION

Before lasers became readily available schlieren, shadowgraph and interferometric methods of optical flow visualisation[1,2] had been widely used in transonic and supersonic wind tunnels. Schlieren and shadowgraph systems, which are sensitive to the first and second derivatives of density respectively, require relatively simple optical arrangements and give results which are excellent for qualitative use but are, in general, unsuitable for quantitative analysis. Conventional interferometers, which are sensitive to density directly, require optical arrangements of extreme accuracy and stability and give results which are good for qualitative use and well suited for quantitative analysis.

The increased availability of lasers with very high spatial and temporal coherence has made possible a number of new interferometer arrangements which were impractical with conventional thermal light sources. In particular a number of interferometer designs based on a conventional schlieren optical system have been proposed and a comprehensive review of these arrangements is presented in Reference 3. The potential importance of a practical interferometer involving only minor changes to a schlieren system is great since many of the transonic and supersonic tunnels in the world are already fitted with schlieren systems while few have interferometric capabilities.

In this note a new schlieren based interferometer design is described which is believed to have characteristics which render it suitable for many practical wind tunnel applications. The results of tests with a prototype based on the ARL transonic wind tunnel schlieren system are also presented.

2. REQUIREMENTS FOR INTERFEROMETERS BASED ON SCHLIEREN SYSTEMS

The main points to be considered when selecting a laser interferometer arrangement based on a schlieren system are:

(i) The mechanical rigidity and vibration isolation of most existing schlieren systems are vastly inferior to the standards required for traditional interferometer designs. Any interferometer design based on a schlieren system must be very insensitive to vibration if it is to have wide application.

The vibration sensitivity of an interferometer appears to be primarily dependent on the separation between the test and reference beams. Interferometers with widely separated beams such as the traditional Mach–Zehnder and Twyman–Green designs[1,2] are extremely vibration sensitive. The minimum vibration sensitivity is exhibited by beam shearing interferometers[3] where each part of the test beam interferes with an adjacent part of the same beam.

(ii) To be useful for wind tunnel applications an interferometer must produce an interferogram which is easily analysed to obtain density and hence the other flow variables at any desired locations in the flow. Traditional designs with separate reference and test beams meet this requirement since the fringe shift is directly related to the density at a particular point in the flow. Except for very small tunnels where the whole schlieren system is mounted on a single rigid base the use of separate reference beams in schlieren based systems is precluded by vibration sensitivity problems. For this reason in all practical schlieren based interferometer designs both the test and reference beams pass through the tunnel test section and the fringe shifts are related to the density difference between two points in the flow. There are two cases where such interferograms are relatively easily analysed.

Firstly, if the reference beam has a very small diameter when it passes through the test section the whole reference beam can be regarded as being subject to a constant

density which if necessary can be measured with a pressure probe. In this case the resulting interferogram can be analysed in the same way as a traditional separate beam interferogram. The second type of interferogram which can be easily analysed is obtained from a beam shearing interferometer with a small shear distance.[3] In this type of interferometer the test and reference beams are effectively slightly displaced parts of the same beam and the fringe shifts are related to local density gradients. These gradients can be integrated from points of known density to obtain the density at any desired point in the flow. All other interferometer types[3] such as those employing large lateral shear, lateral inversion, angular shear or linear compressive shear give interferograms which are difficult to analyse.

(iii) Transonic flows are often very unsteady and experience has shown that exposure times of the order of 1μ second are necessary to obtain sharp unblurred flow visualisation pictures. To produce interferograms at these short exposure times using normal photographic films a continuous laser of at least 1 watt or a Q switched solid state laser is required. The optics of any practical interferometer must therefore be sufficiently robust to avoid damage from either of the above laser types.

In practice this requirement precludes the use of diffraction gratings or cemented optical components near focal points.

(iv) Because the main features of a compressible flow, such as the occurrence of shock waves and boundary layer separations, are more clearly shown by schlieren pictures, than by interferograms, both systems should be available as they are complementary to one another. In view of this requirement it is desirable that only minor alterations to the schlieren optical system be required to produce the interferometer so that changes between the two systems can be made quickly and easily.

3. PRELIMINARY INVESTIGATION OF EXISTING DESIGNS

When the published schlieren based interferometer designs[3] are considered in the light of the requirements listed in the previous section it is evident that most of them can be eliminated from serious consideration for practical wind tunnel applications. Overall the most promising arrangements appear to be the reflection plate beam shearing designs described originally in References 4 and 5. Of the two the Murty–Tanner design of Reference 4 is the simpler and since it has no obvious disadvantages it was selected for more detailed investigation. Using the ARL transonic wind tunnel schlieren system (described in Appendix A) as a basis, a Murty–Tanner interferometer was constructed and tested (Appendix B). The main conclusions from these tests are:

(i) Laser interferometers based on schlieren systems can give good quality interferograms despite the problems of mechanical stability, reflections from tunnel windows and scattering from imperfect optical components.

(ii) Beam shearing interferometers involve a trade off between spatial resolution and sensitivity. For tunnels of relatively small size and low operating pressure this compromise leads to results of low accuracy. It appears that beam shearing interferometers would only be really attractive for tunnels where the parameter [tunnel width × stagnation pressure] exceeded about 750 kPa m.

It appears that none of the schlieren based interferometer designs proposed up to now are entirely suitable for the majority of small and medium size wind tunnels. This view is supported by the fact that despite over 10 years development there does not seem to be any published aerodynamic investigation where a laser interferometer based on a schlieren system has been used to obtain quantitative measurements.

4. THE NEW INTERFEROMETER

4.1 General Description

The basic arrangement of the most common wind tunnel schlieren system is presented in Figure 1. The modifications to produce the proposed interferometer are shown schematically in Figures 2 and 3. A laser with a standard microscope objective-pin hole beam expander is

used as a light source. A lens of suitable diameter and focal length (see next section) is introduced between the light source and the collimating mirror so that a portion of the light which would otherwise form the collimated beam through the test section is brought to a focus on the tunnel midplane. The lens is used off the mirror axis so that the focal spot is displaced away from the centre of the field of view where the model would be located. The light captured by the lens and focused on the tunnel midplane forms the reference beam and the light not obstructed by the lens forms the test beam. By selecting a suitable lens it can be arranged that approximately half the original beam is unobstructed and that most of the remaining light is captured by the lens to form the reference beam (Fig. 2).

At the receiving end of the system (Fig. 3) another lens is used to intercept the reference beam and form a source image coincident with the source image formed by the test beam. A plane mirror with its leading edge adjacent to the source image and approximately parallel to the focusing mirror centreline is used to fold the reference beam back onto the scene beam. The angle of this plane mirror is adjusted so that the scene and reference beams are superimposed in the test section image plane. The angle of recombination of the two beams and hence the fringe spacing in the region of overlap is dependent on the distance between the plane mirror and the focusing mirror centreline. As this distance is increased the fringe spacing is reduced.

When the tunnel is operating the source images formed by the test beam and to a lesser extent the reference beam will be blurred by refraction caused by density gradients in the flow. If the plane mirror is placed too close to the focusing mirror axis its leading edge will cut off some of the refracted light and unwanted schlieren effects will appear in the resulting interferogram. For this reason the proposed interferometer is inherently more suited to the production of fine finite fringe interferograms than near infinite fringe interferograms.

If "no flow" and "with flow" fine finite fringe interferograms are superimposed a new set of composite moiré fringes become visible. These fringes which are analogous to those observed in an infinite fringe interferogram are lines of constant density. This superposition technique has the major advantage that disturbances present in both interferograms are cancelled out. Therefore mirrors, lenses and tunnel windows of low quality can be used without affecting the accuracy of the final composite interferogram. This technique has been used in the past with non-laser interferometers[7,8] but in these cases the resolution of the composite fringes was poor due to the limited number of clear fringes in the original interferograms imposed by the relatively large spectral bandwidth of the source.[9] This resolution limitation is not a problem with a laser light source.

The reference beam geometry employed, with a waist at the tunnel midplane, has the important advantage that a first order concellation occurs of density gradients across the beam. This feature can be illustrated by considering a fairly small diameter reference beam passing through a locally linearised two dimensional density field (Fig. 6). Consider a ray within the reference beam entering the tunnel at a point x_1, z_1.The co-ordinates of any point on this ray are given by:

$$x = x_1\left(1 - \frac{2y}{b}\right)$$

$$z = z_1\left(1 - \frac{2y}{b}\right)$$

The density (ρ) at any point near the reference beam axis is given by:

$$\rho = \rho_0 + x\frac{\partial \rho}{\partial x} + z\frac{\partial \rho}{\partial z}$$

The fringe shift (δN) due to the density field is given by:

$$\delta N = K\int_0^b \rho \, dy$$

where K is a constant depending on the wavelength of the light used.

From the above equations

$$\delta N = K \int_0^b \left[\rho_0 + x_1 \left(1 - \frac{2y}{b}\right) \frac{\partial \rho}{\partial x} + z_1 \left(1 - \frac{2y}{b}\right) \frac{\partial \rho}{\partial z} \right] dy$$

$$= K \left[\rho_0 y + x_1 \left(y - \frac{y^2}{b}\right) \frac{\partial \rho}{\partial x} + z_1 \left(y - \frac{y^2}{b}\right) \frac{\partial \rho}{\partial z} \right]_{y=0}^{y=b}$$

$$= K \rho_0 b$$

It is evident from this that for a small but finite reference beam traversing a two dimensional density field with linear density gradients each ray in the beam experiences a constant fringe shift. Similar but less complete density gradient cancellation occurs for symmetrical three dimensional density fields such as those generated by unyawed aircraft models. Although no detailed analysis has been carried out it appears that refraction effects should be no worse with a waisted beam than with a collimated beam.

4.2 Detail Design

The operation of this interferometer depends primarily on the selection and location of the two lenses. The requirements for the lenses will be developed considering the source optics (reproduced diagramatically in Figure 4 with the reference beam focusing lens on the mirror centreline for simplicity).

The parameters to be determined are:

F_l = Focusing lens focal length;

d_l = Focusing lens diameter;

x_l = Distance from collimating mirror axis to focusing lens optical centre;

U_l = Distance from source to focusing lens.

The known parameters are:

F_m = Collimating mirror focal length;

V_m = Distance from collimating mirror to tunnel centreline;

x = Distance from tunnel centreline to reference beam waist.

Other parameters that will be used during derivation:

V_l = Distance from focusing lens to virtual image of source;

U_m = Distance from collimating mirror to virtual image of source formed by focusing lens;

d_m = Diameter of reference beam at collimating mirror;

d_w = Diameter of reference beam at tunnel sidewall.

The sign convention used is shown in Figure 4.

Unfortunately it is not possible to derive explicit expressions for the quantities to be determined but relationships to assist in their rational selection will be developed.

From the general mirror equation:

$$\frac{1}{V_m} + \frac{1}{U_m} = \frac{1}{F_m} \tag{1}$$

and from the thin lens equation

$$-\frac{1}{V_l} + \frac{1}{U_l} = \frac{1}{F_l} \tag{2}$$

From Figure 4 it can be seen that

$$V_1 - U_1 = U_m - F_m \tag{3}$$

From equations (1), (2) and (3) it can be shown that:

$$F_1 = \frac{U_1^2 (V_m - F_m) + U_1 F_m^2}{F_m^2} \tag{4}$$

N.B. When using this equation to calculate the value of U_1 for a given F_1 the positive root is the relevant one.

From Figure 4 it can be seen that:

$$d_m = d_1 \cdot \frac{U_m}{V_1} \tag{5}$$

Using equations (1) and (2) to eliminate the unknowns U_m and V_1 from equation (5) we obtain:

$$d_m = d_1 \cdot \frac{F_m V_m}{V_m - F_m} \cdot \frac{F_1 - U_1}{U_1 F_1} \tag{6}$$

From Figure 4:

$$d_w = d_m \cdot \frac{b}{2V_m} \tag{7}$$

Combining equations (6) and (7) we obtain:

$$d_w = d_1 \cdot \frac{bF_m}{2U_1 F_1} \cdot \frac{F_1 - U_1}{V_m - F_m} \tag{8}$$

Since the ray passing through the optical centre of the lens is not deflected, the reference beam can be moved away from the tunnel centreline by simply moving the reference beam focusing lens off the mirror centreline. From Figure 4 it can be seen that:

$$x = x_1 \cdot \frac{F_m}{U_1} \tag{9}$$

The derivation of the above equations was carried out for $V_m > F_m$ (which is the case for most schlieren systems). If $V_m < F_m$ the reference beam focusing lens would be required to form a real image of the source beyond the collimating mirror and V_1 and U_m would change sign. These sign changes do not affect any of the above equations and they are applicable in both cases. The above analysis is also directly applicable to the receiving end optics.

The arrangement giving the maximum usable interferogram coverage, and hence the most desirable arrangement for most applications, is shown in Figure 5. The suggested procedure for achieving this desirable arrangement without resorting to expensive custom made lenses is as follows:

(i) Select a mechanically convenient location between the source and the collimating mirror to mount the reference beam focusing lens. To keep the lens size to a readily available value the beam diameter where the lens is inserted should be in the range 20 mm to 160mm.

(ii) Using equation (4) calculate the lens focal length F_1.

(iii) From a lens suppliers catalogue select a lens with a focal length near the calculated value and a diameter slightly less than half the beam diameter at the desired insertion point.

(iv) Use equations (4), (6) and (9) with the actual values of lens diameter and focal length calculate U_1, d_m and x_1. Using these values check that the proportion of the test beam cut off by the lens is acceptable and that the reference beam does not overlap the edge of the collimating mirror.

(v) If the arrangement is unsatisfactory select another lens and repeat (iv).

If the schlieren system is symmetrical about the tunnel test section [i.e. V_m (source end) = V_m (receiving end)] identical lenses at the same value of U_1 (measured from the source image at the receiving end) can be used for the reference beam focusing and expanding lenses. If the

schlieren system is not symmetrical about the test section, as is the case for the ARL transonic tunnel system (Fig. 7), the following procedure is suggested.

(i) Select a suitable reference beam focusing lens as described above.

(ii) Using equation (4) calculate F_1 for the reference beam expanding lens assuming the same value of U_1 as for the focusing lens.

(iii) From a catalogue of standard lenses select one which has the same diameter as the focusing lens and a value of F_1 as near as possible to that calculated in step (ii).

(iv) Using the selected value of F_1 calculate U_1 and x_1 for the beam expanding lens from equations (4) and (9).

The beam folding mirror (Fig. 3) has no special requirements except that it be front surfaced and of adequate size to reflect the complete reference beam. If it were more convenient the test beam could equally well be folded onto the reference beam.

It should be noted that since the reference beam area is less than the test beam area, an interferogram covering the whole test beam is not obtained (Fig. 5). However, by adjusting the angle of the beam folding mirror and the lateral position of the beam expanding lens the reference beam may be superimposed on any desired portion of the test beam.

4.3 Summary of Features

The interferometer design described here has the following significant features:

(i) The conversion of a standard schlieren system to this interferometer arrangement involves only the provision of a suitable laser light source (see (v) and (vi) below), the removal of the knife edge and the addition of two lenses and a plane mirror. The optical quality of these added components is not critical.

(ii) The optical arrangement is very robust and no difficulties should be experienced in using high power continuous lasers or Q switched pulsed lasers.

(iii) Since the test and reference beams follow very similar paths and are reflected from the same collimating and focusing mirrors the vibration sensitivity should be low.

(iv) Due to the small diameter of the reference beam, its large displacement from the centre of the field of view and the density gradient cancellation, it should be possible to regard the entire reference beam as being subject to a constant fringe shift. This greatly simplifies the analysis of the resulting interferograms.

(v) The path lengths of the test and reference beams are very similar and no difficulties should be experienced with fringe contrast provided the coherence length of the laser used significantly exceeds the thickness of the reference beam focusing and expanding lenses. Lasers with very poor temporal coherence may require the use of a plane glass plate in the test beam to compensate for the two lenses in the reference beam.

(vi) Due to the geometry of the beam folding used, the laser output only requires to be coherent over slightly more than half the beam diameter.

The main disadvantage of the proposed arrangement is that only slightly less than half of the original schlieren beam area is available. In many cases this is not a serious problem since only a portion of the flow field is of interest. However, if necessary two separate interferograms with the model upright and inverted will cover almost the entire field. The inability of the proposed system to produce a finite fringe interferogram with initially straight fringes may also be a disadvantage in some circumstances.

5. PROTOTYPE INSTRUMENT

5.1 Description

A prototype interferometer was constructed using the transonic tunnel schlieren system (Fig. 7 and Appendix A) as a basis. To fit the 15 mW He–Ne laser used for these tests into the limited space between the plenum chamber and the return leg of the tunnel the source optics had to be slightly altered (Fig. 8). The beam expanding arrangement shown in this figure was used because the components were readily available. It would in fact have been preferable to use a higher power microscope objective and dispense with the concave lens following the pin hole.

A pair of cemented achromatic doublets 60 mm diameter and 480 mm focal length were used for the reference beam focusing and expanding lenses. The beam folding mirror was a

front silvered piece of plate glass 145 mm wide and 460 mm long. Both the lenses and the mirror were selected because of their availability not because they were in any way optimum for this application. To facilitate adjustment of the system the lenses were stuck in place with lumps of "plasticine" (suitable multi-degree of freedom optical mounts not being available) and the mirror was suspended from three adjusting screws. The location of the reference beam focusing lens is shown in Figure 8. The reference beam expanding lens was located between the third and fourth plane mirrors (Fig. 7) fortunately in a position where it did not obstruct either the test or reference beams. The use of identical lenses at both ends of the system instead of the optimum arrangement for the asymmetrical system (section 4.2) resulted in some loss of reference beam light at the receiving end of the system. The different intensities in the test and reference beam would be expected to reduce the fringe contrast but in this case the problem did not appear to be serious.

A 2¼" square single lens reflex camera with the lens removed was used to record the interferograms and 400 ASA panchromatic film was used for all tests. The exposure was set with a simple spring loaded slit shutter located near the leading edge of the beam folding mirror. The focal plane shutter fitted to the camera was used simply as a capping shutter to prevent fogging between exposures. It was found that good images approximately 50 mm diameter could be obtained at an exposure time of 300 μs. The camera and the spring loaded shutter were mounted on a separate support which simply stood on the floor alongside the shockmounted framework which supported the rest of the optics. This was found to be necessary to prevent vibration due to camera and spring loaded shutter actuation causing fringe blurring.

5.2 Adjustment Procedure

Based on the experience gained with the prototype instrument the following setting up procedure is suggested:

(i) Select suitable optical components to expand the laser beam. If a microscope objective is used it is essential to use a pin hole spatial fitter at its focal point to remove the resulting noise. However, if scrupulously clean unscratched single element lenses are used good results can be achieved without spatial filtering. Due to the Gaussian intensity distribution of laser beams it is best to overexpand the beam and reflect only the inner, higher intensity, portion of the beam from the collimating mirror.

(ii) As with a schlieren system adjust the source position and the collimating mirror to produce a properly collimated beam aligned in the desired direction. Adjust the focusing mirror so that the source image occurs at the desired location.

(iii) Introduce the reference beam focusing lens (Fig. 2) into the system at the location calculated as described in section 4.2. Place a white screen on the tunnel centreline and make fine five axis (all degrees of freedom except rotation about optical axis) adjustments to the lens until the smallest possible undistorted spot is obtained on the screen at the desired reference beam location. Remove the screen and check that the reference beam is of the same size and shape at the entrance and exit windows, if not carry out further lens adjustments. If the reference beam covers any scratches or chips in the tunnel windows move it slightly to avoid these defects.

(vi) Introduce the reference beam expanding lens (Fig. 3) into the system at the location calculated by the method of section 4.2. Make five degree of freedom adjustments to the lens until the best possible reference beam source image coincides with the test beam source image. In all conventional schlieren systems (except those using lenses or off axis paraboloidal mirrors) the source image formed by the test beam will suffer some degree of astigmatism. The source image formed by the reference beam will be fairly free of this aberration due to the small size of this beam. If the astigmatism is significant it is suggested that the reference beam be focused in the middle of the line image which lies parallel with the beam folding mirror. This procedure minimises the mirror offset required to avoid schlieren cut off effects.

(v) Focus the image of the test region formed by the test beam onto the camera film plane using a suitable lens if necessary. Fine focusing is best done by operating the tunnel and moving the camera and/or lens until shadowgraph effects are minimised. Attempts at

focusing by other methods are frustrated by the large depth of field caused by the very small source size.

(vi) Insert the beam folding mirror (Fig. 3) with its leading edge aligned with the line of the astigmatic source image which is parallel to the mirror. Adjust the angle and offset of the mirror to produce the desired fringe spacing and overlap between the two beams. If the fringes are significantly curved they can be centred by a small transverse movement of the reference beam expanding lens.

5.3 Test Results

The interferometer was set up and adjusted as described in sections 5.1 and 5.2. A 101·6 mm chord model of supercritical aerofoil BGK-1[9] which completely spanned the width of the tunnel was mounted between glass windows. The interferogram was centred on the upper surface of the aerofoil since this was the region of major aerodynamic interest.

The no flow fringes were found to have significant curvature. This curvature was reduced, as the fringe spacing was reduced, by increasing the beam folding mirror offset (Figs 9, 10 and 11). The total number of fringes across the interferograms illustrated in Figures 9, 10 and 11 are 100, 200 and 400 respectively. Test interferograms with up to 1200 fringes were produced but beyond 400 the fringe contrast was found to steadily deteriorate. The 400 fringe interferograms were produced with a beam folding mirror offset of approximately 2 mm. Since this offset was sufficient to avoid most schlieren cut off problems it was used for all further tests. The dark region near the leading edge in the with flow interferogram of Figure 11 is due to vestiges of the schlieren effect.

To assess the mechanical stability of the system a number of no-flow interferograms were recorded and superimposed in pairs. This superposition produced from one to five background fringes covering the field (Fig. 12). An unavoidable uncertainty of about five fringes across the field will therefore apply to all superimposed interferograms due to mechanical unsteadiness of the system. These background moiré fringes tended to be predominantly oriented parallel to the initial fringes suggesting that they were caused by changes in the initial fringe spacing rather than fringe shape or angle. In Figure 12 the sensitivity of the interferogram superposition to angular and chordwise misalignment is illustrated. Moderate misalignment normal to the chord did not produce any fringes. The sensitivity to angular misalignment increases with decreasing fringe spacing while the sensitivity to chordwise misalignment increases with increasing fringe curvature (i.e. increasing fringe spacing). For the tests reported here alignment errors were estimated to contribute less than one fringe over the whole field.

A number of composite moiré fringe interferograms of the flow over the upper surface of the aerofoil were produced (Figs 13–18) Due to the long exposure time required by the low power laser used, fringe blurring occurred in unsteady flow regions. The interferograms where the fringe legibility was insufficient for direct photographic reproduction are reproduced in the form of fringe tracings (Figs 15–18) Where the fringes were completely illegible in the original composite interferogram but their location could be reasonably inferred they are shown as broken lines. Locations where apparently physically unrealistic fringe discontinuities occur are marked with a question marks It is considered that these fringe discontinuities are also caused by the long exposure time used.

The interferograms in Figures 13–18 exhibit good qualitative agreement with the known nature of the flow over this aerofoil section. For these results there is little difficulty in inferring the sign of the density change between adjacent fringes. In more complex flows this can be determined from the direction of fringe movement in the original finite fringe "with flow" interferogram. For example in the "with flow" interferogram of Figure 11 the fringes are displaced upwards in regions of reduced density.

Since an experimental surface pressure distribution was available[9] for the same test conditions as the interferogram in Figure 16, this interferogram was selected for quantitative analysis. From Reference 8:

$$\frac{P}{H} = \left[\left(\frac{P_r}{H} \right)^{1/\gamma} + \frac{\lambda R T_0}{k L H} \cdot N \right]^{\gamma}$$

where P = static pressure at any point

H = tunnel stagnation pressure

P_r = reference pressure

T_0 = tunnel stagnation temperature

L = tunnel width

R = gas constant

k = Gladstone–Dale constant

λ = wavelength of light used

γ = ratio of specific heats

N = fringe number where P is required (P_r is measured on fringe zero)

Two surface pressures were measured on the aerofoil at $x/c = 0{\cdot}117$ and $0{\cdot}854$. Using these two pressures and the total number of fringes between the two points (the surface pressure being known to vary monotonically between these points) the value of the constant $\lambda RT_0/kLH$ was calculated from the above equation. This procedure avoided the errors which would otherwise have been introduced by the sidewall boundary layers.

The measured pressure at $x/c = 0{\cdot}117$ was defined as P_r in the above equation which was then used to calculate P at each intersection between a fringe and the aerofoil surface. The result of this analysis is presented in Figure 19. As mentioned previously the background fringes caused by vibration were predominantly parallel to the aerofoil surface and would not therefore contribute errors to the above analysis.

Surface pressure measurements for the same conditions ($M = 0{\cdot}763$, $\alpha = 1{\cdot}4^\circ$) from Reference 9 are plotted in Figure 19. To illustrate the sensitivity of the flow to small changes in Mach number a pressure distribution for $M = 0{\cdot}761$, $\alpha = 1{\cdot}4^\circ$ is also plotted. Considering the extreme sensitivity of the flow to Mach number changes Figure 19 shows good agreement between the interferometric and pressure measurement data.

6. CONCLUSION

A new laser interferometer based on a conventional wind tunnel schlieren system has been designed and tested. This interferometer design has the following favourable features:

(i) The optical arrangement is very simple requiring only the addition of a suitable laser light source, two lenses and a plane mirror to a standard schlieren system.

(ii) It is optically robust and no difficulties should be experienced using high power CW or Q switched lasers.

(iii) The vibration sensitivity is low since the scene and reference beams follow similar paths.

(iv) The design imposes only moderate requirements on the temporal and spatial coherence of the laser used.

(v) The reference beam is of small diameter and passes through the test section at a point well removed from the model location. This feature greatly assists the analysis of the interferograms.

(vi) The interferograms produced are well suited to the superposition technique of cancelling optical system imperfections.

The main disadvantage of the design is that slightly less than half of the total field of view is available. However, the whole field may be covered by taking multiple interferograms. The inability of this interferometer to produce a finite fringe interferogram with initially straight fringes may also be a disadvantage in some circumstances.

The ARL transonic wind tunnel schlieren system used for the prototype tests has an unusually large number of beam folding mirrors, four schlieren quality glass windows in the test beam and relatively low mechanical rigidity due to the separate mounting of the source and receiving optics assemblies.

All of these characteristics, while perfectly satisfactory for the original purpose of the system, mitigate against the successful realisation of the interferometer. The fact that good

quality interferograms were obtained from the prototype suggests that this interferometer arrangement could be used successfully with many existing wind tunnel schlieren systems.

REFERENCES

1.	Holder, D. W., North, R. J., and Wood, G. P.	Optical Methods for Examining the Flow in High-Speed Wind tunnels. AGARDograph 23. 1956
2.	Weinberg, F. J.	Optics of flames. Butterworth. 1963.
3.	Tanner, L. H.	The Design of Laser Interferometers for Use in Fluid Mechanics. J. Sci. Inst., 1966, Vol. 43, pp. 878–86.
4.	Tanner, L. H.	Some Laser Interferometers for Use in Fluid Mechanics. J. Sci. Inst., 1965, Vol. 42, pp. 834–37.
5.	Oppenheim, A. K., Urtiew, P. A., and Weinberg, F. J.	On the Use of Laser Light Sources in Schlieren–Interferometer Systems. Pro. Roy. Soc. A, 291, 1966, pp. 279–90.
6.	Ashkenas, H. L., and Bryson, A. E.	Design and Performance of a Simple Interferometer for Wind Tunnel Measurements. J. Aero. Sci., Vol. 18, No. 2, Feb. 1951.
7.	Bryson, A. E.	An Experimental Investigation of Transonic Flow Past Two-Dimensional Wedge and Circular Arc Sections Using a Mach–Zehnder Interferometer. NACA Tech. Note 2560. 1951.
8.	Tanner, L. H.	The Design and Use of Interferometers in Aerodynamics. ARC R & M 3131. Sept. 1957.
9.	Pollock, N., and Fairlie, B. D.	An Investigation of Supercritical Aerofoil BGK-1. Part 1: Near Design Point Tests and Comparisons with Theory. ARL Aero. Report 144. Nov. 1975.
10.	Pollock, N.	Lasers for Transonic Tunnel Flow Visualisation—A Preliminary Survey. ARL Aero. Tech. Memo 285. Sept. 1974.

APPENDIX A

Description of Transonic Tunnel Schlieren System

The ARL transonic tunnel is a conventional continuous closed circuit facility. The test section, which is 533 mm wide and 813 mm high, is surrounded by a 2·54 m diameter pressure shell. The tunnel Mach number range is 0·5 to 1·4. The maximum stagnation pressure (which is limited by the available drive power) varies from 100 kPa for Mach numbers up to 0·6 to 23 kPa at $M = 1{\cdot}4$.

The tunnel is equipped with a permanently installed 406 mm aperture schlieren system, a scale drawing of which is presented in Figure 7. Due to the limited space available between the test section pressure shell and the return leg of the tunnel the optical path of the source end optics is folded with a pair of plane mirrors. Similarly, to save space in the tunnel control room, the receiving optics also employ a folded configuration. All the mirrors are front aluminized and all except the two 406 mm diameter spherical mirrors are quartz coated. The two test section windows and the two pressure shell windows have surfaces which are flat to within 0·025 λ/mm (where $\lambda = 590$ nm for sodium light) and parallel to within 5 minutes. None of the window surfaces is anti-reflection coated. The source and receiving optics assemblies are mounted on separate tubular steel frames fitted with soft rubber shock mounts which rest on the concrete floor slab. The natural vibration frequencies of the two optics assemblies appear to be less than 10 Hz. The relative displacements between the two optics assemblies due to vibration during tunnel operation have not been accurately measured but are believed to be of the order of 0·2 mm horizontally and somewhat less vertically.

APPENDIX B

Tests on Murty-Tanner Interferometer

The transonic tunnel schlieren system was converted to a Murty–Tanner beam shearing interferometer (Fig. 20) as follows:

The original light source was replaced with a 15 mW continuous He–Ne gas laser, the output beam of which was expanded using a microscope objective and pin hole spatial filter. The knife edge was removed and a glass plate approximately 20 mm diameter and 2 mm thick was introduced just past the knife edge location, inclined at approximately 45° to the incident beam. The front and rear reflections from the glass plate were focused to produce two slightly displaced images on the film plane of a camera.

On completion of the set up clear interference fringes of high contrast were immediately obtained. Previous laboratory tests carried out at ARL[10] had shown that the shear distance and the fringe spacing could be varied independently by using slightly non-parallel glass reflection plates. A plate was selected which gave a shear distance of approximately 9 mm and a convenient initial fringe spacing ($\simeq 240$ fringes across the field of view). A two dimensional aerofoil model completely spanning the width of the tunnel was used for these tests. An exposure time of 1 m sec (the fastest shutter speed available) was found to give a good exposure with an image approximately 50 mm diameter on 400 ASA panchromatic film. In Figure 21 "with flow" and "no flow" interferograms are presented with the shear parallel to the aerofoil chord giving fringe shifts proportional to chordwise density gradients.

From Figure 21 it can be seen that the "no flow" interferogram has fringes of high contrast with relatively little background noise. This indicates that scattering from the large number of mirror surfaces in the transonic tunnel schlieren system and multiple reflections from the four windows in the beam does not prevent the formation of good quality laser interferograms. The fringes in the "with flow" interferogram are somewhat patchy due to flow unsteadiness and the relatively long exposure time used. However, the fact that good fringes are obtained in regions where steady flow would be expected (e.g. upstream of the model) indicates that the mechanical stability of the arrangement was adequate.

An attempt to quantitatively analyse the interferograms of Figure 21 showed that away from the leading edge region the fringe shifts were too small to be accurately measured. This low accuracy density gradient information led to gross inaccuracies in the resulting integrated density and pressure data. Increasing the beam shear increased the fringe shifts but the analysis became unacceptably complicated because the fringe shifts could no longer simply be regarded as being caused by local density gradients. On the basis of experience gained during the current tests it appears that beam shearing interferometers would only be really useful on large high pressure tunnels, i.e. the parameter [model size × tunnel pressure] more than an order of magnitude larger.

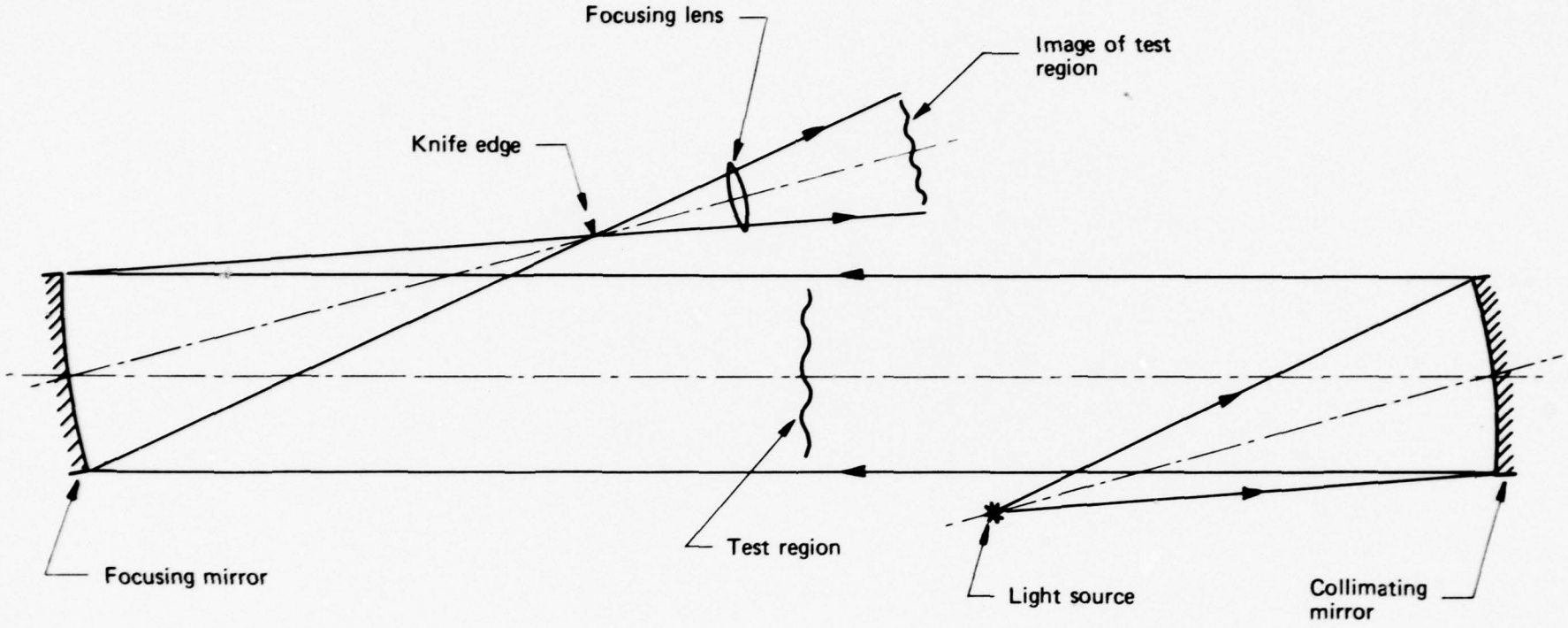

FIG. 1 ARRANGEMENT OF BASIC SCHLIEREN SYSTEM

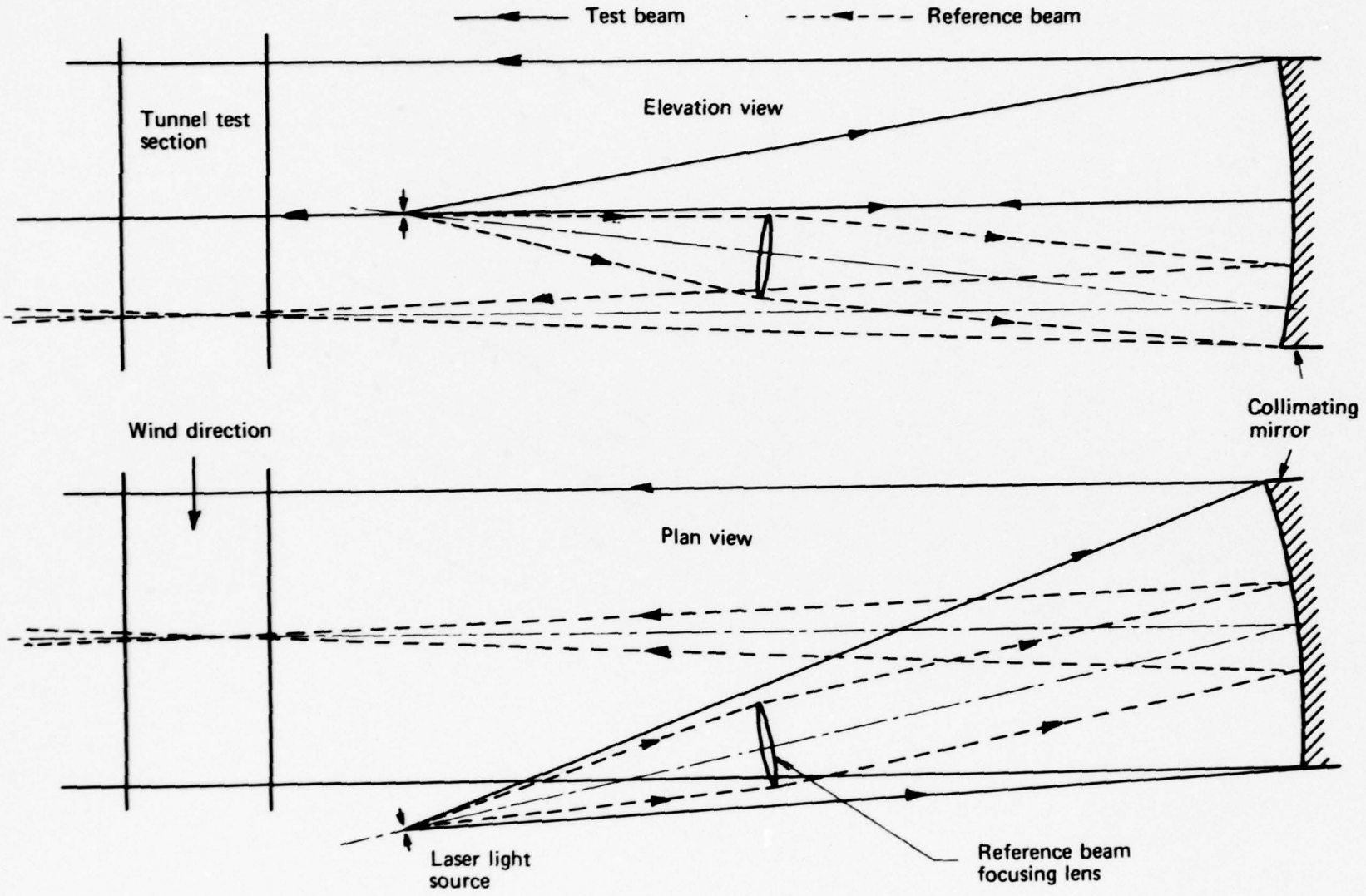

FIG. 2 ARRANGEMENT OF INTERFEROMETER (Source end)

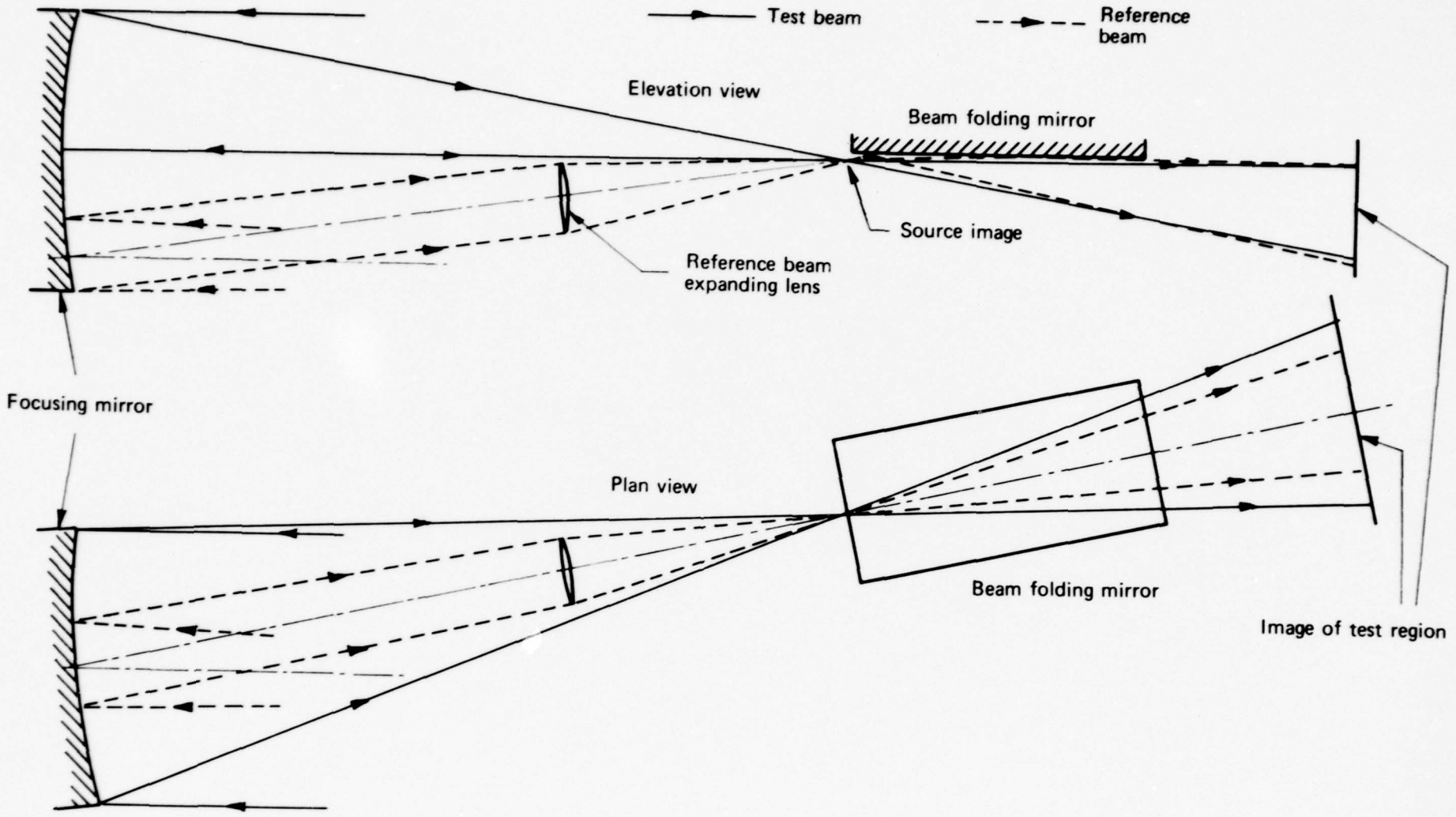

FIG. 3 ARRANGEMENT OF INTERFEROMETER (Receiving end)

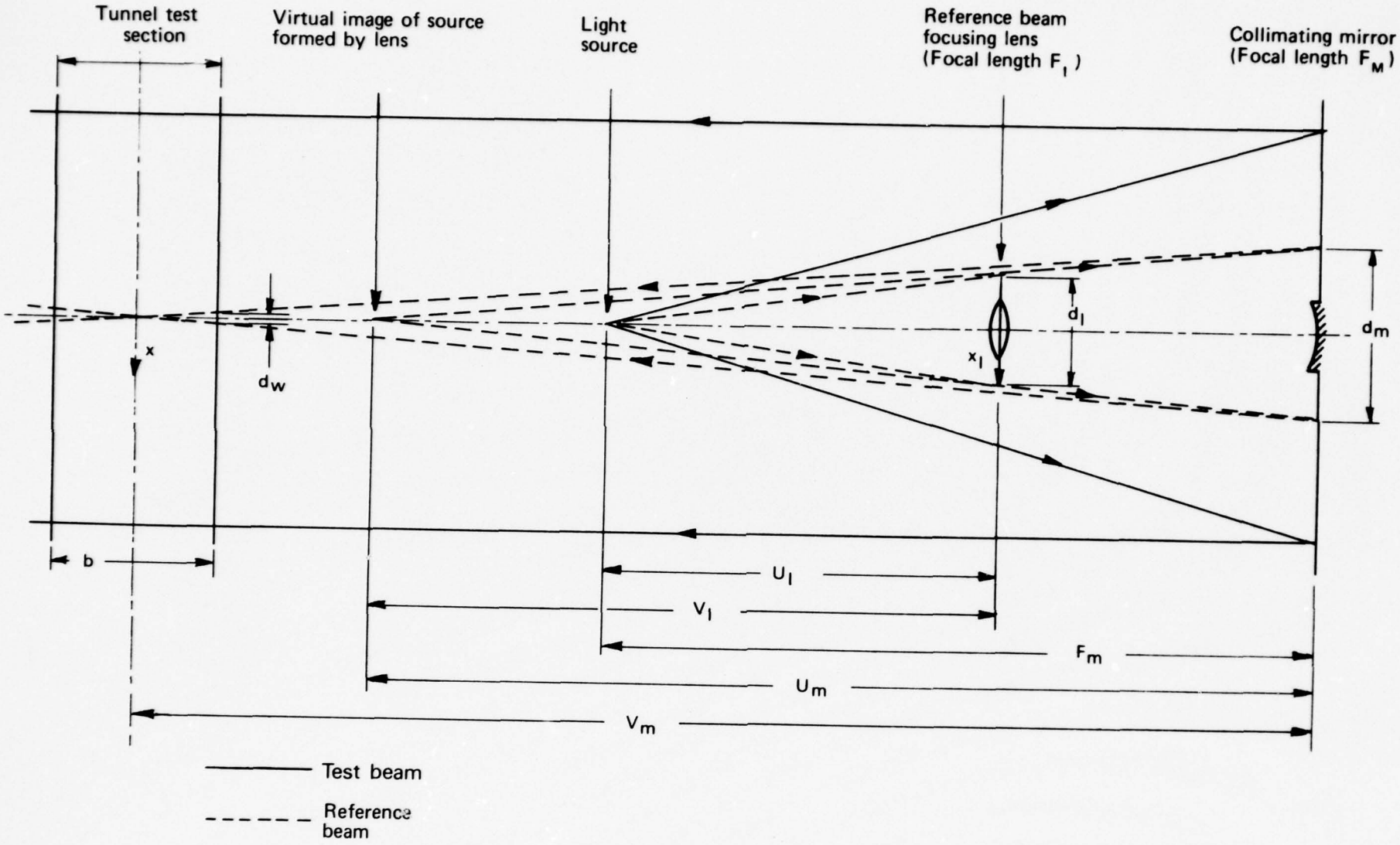

FIG. 4 GEOMETRY OF SOURCE OPTICS OF INTERFEROMETER

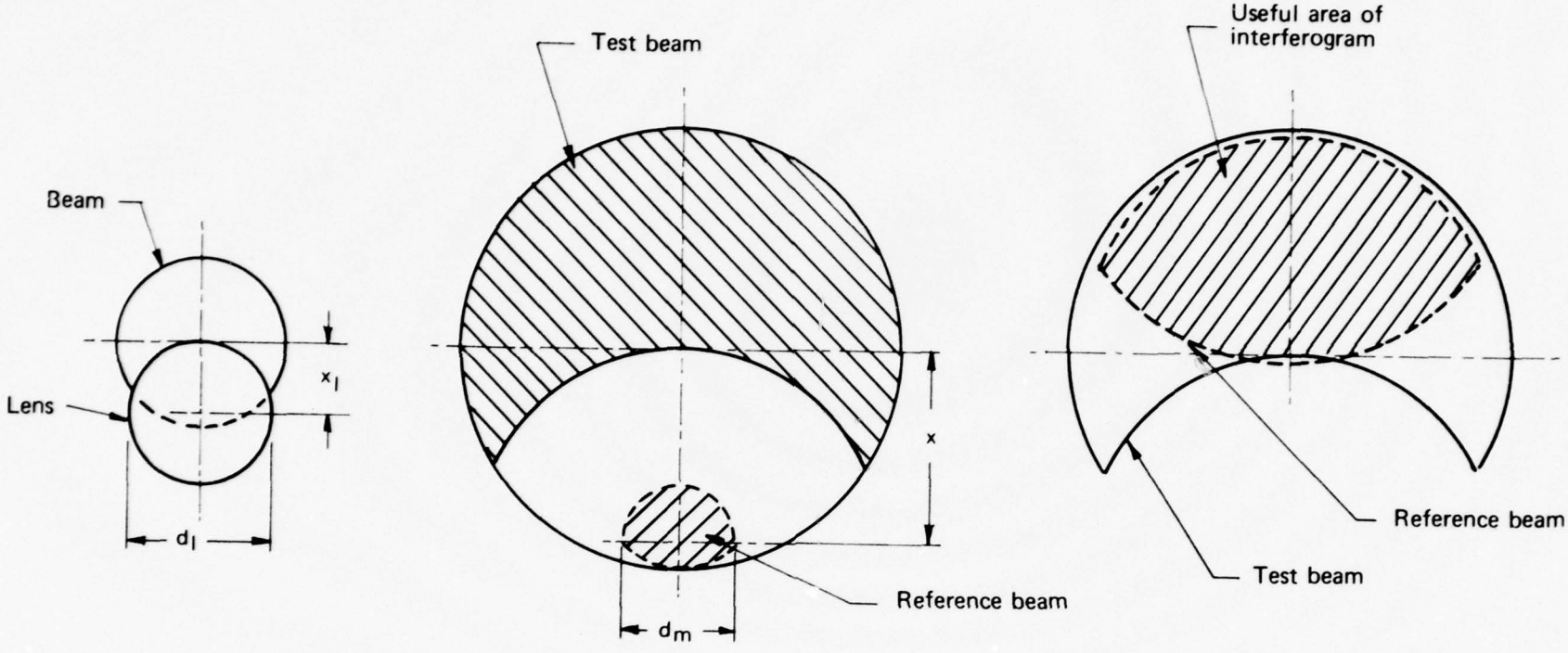

Section through plane of reference beam focusing lens

Section at collimating mirror

Test section image plane

FIG. 5 OPTIMUM ARRANGEMENT OF REFERENCE BEAM
(Circular reference beam focusing lens)

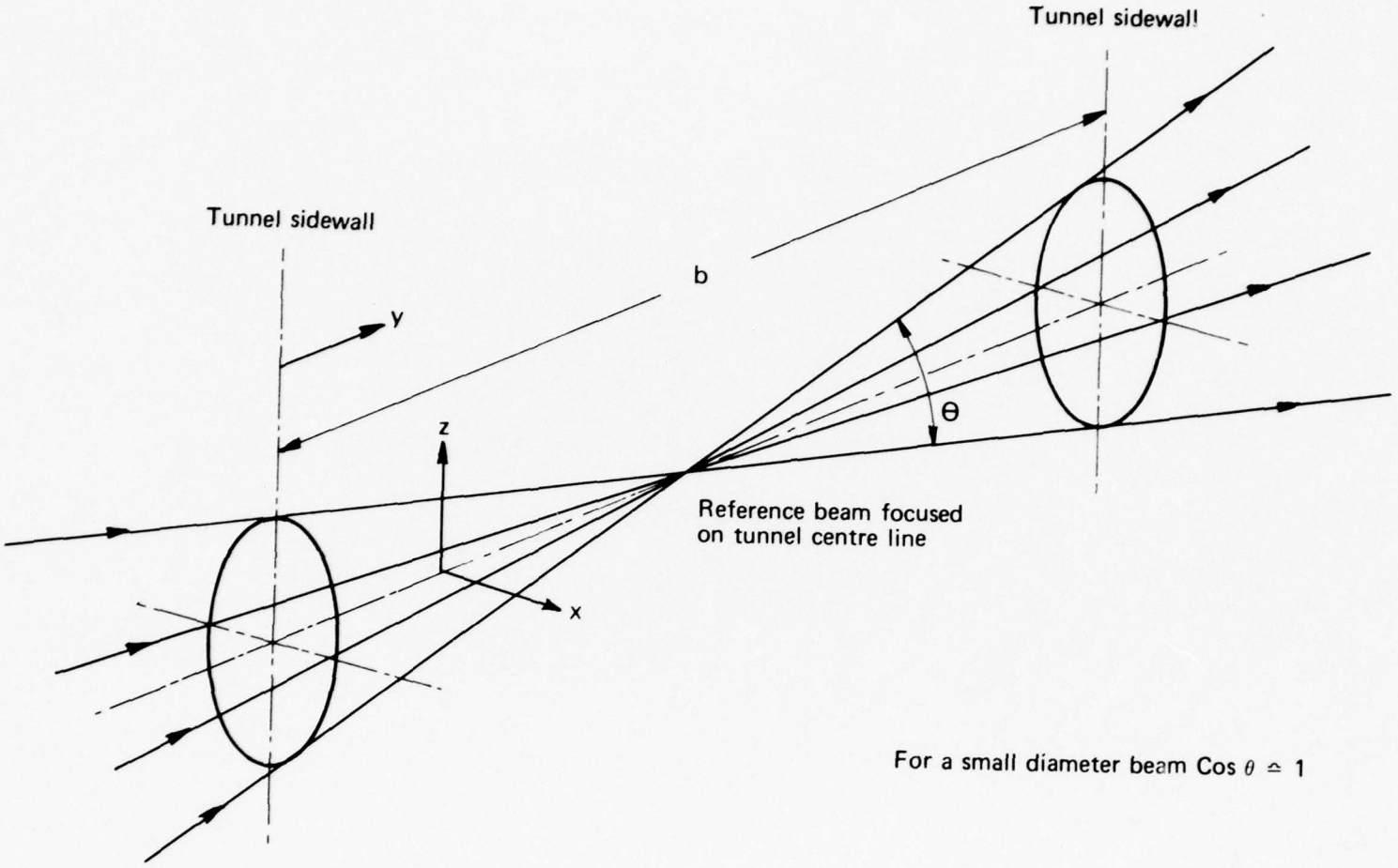

FIG. 6 GEOMETRY OF REFERENCE BEAM IN TUNNEL TEST SECTION

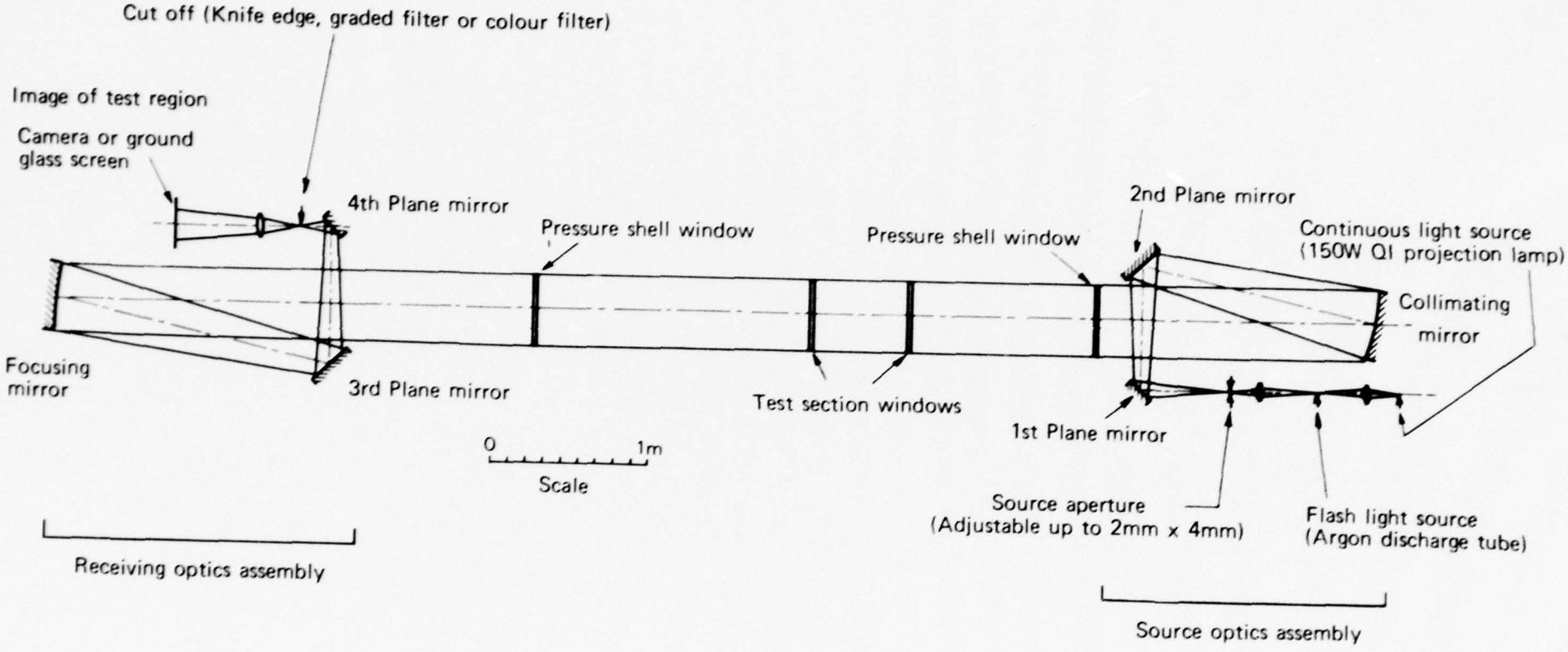

FIG. 7 DETAILS OF TRANSONIC TUNNEL SCHLIEREN SYSTEM

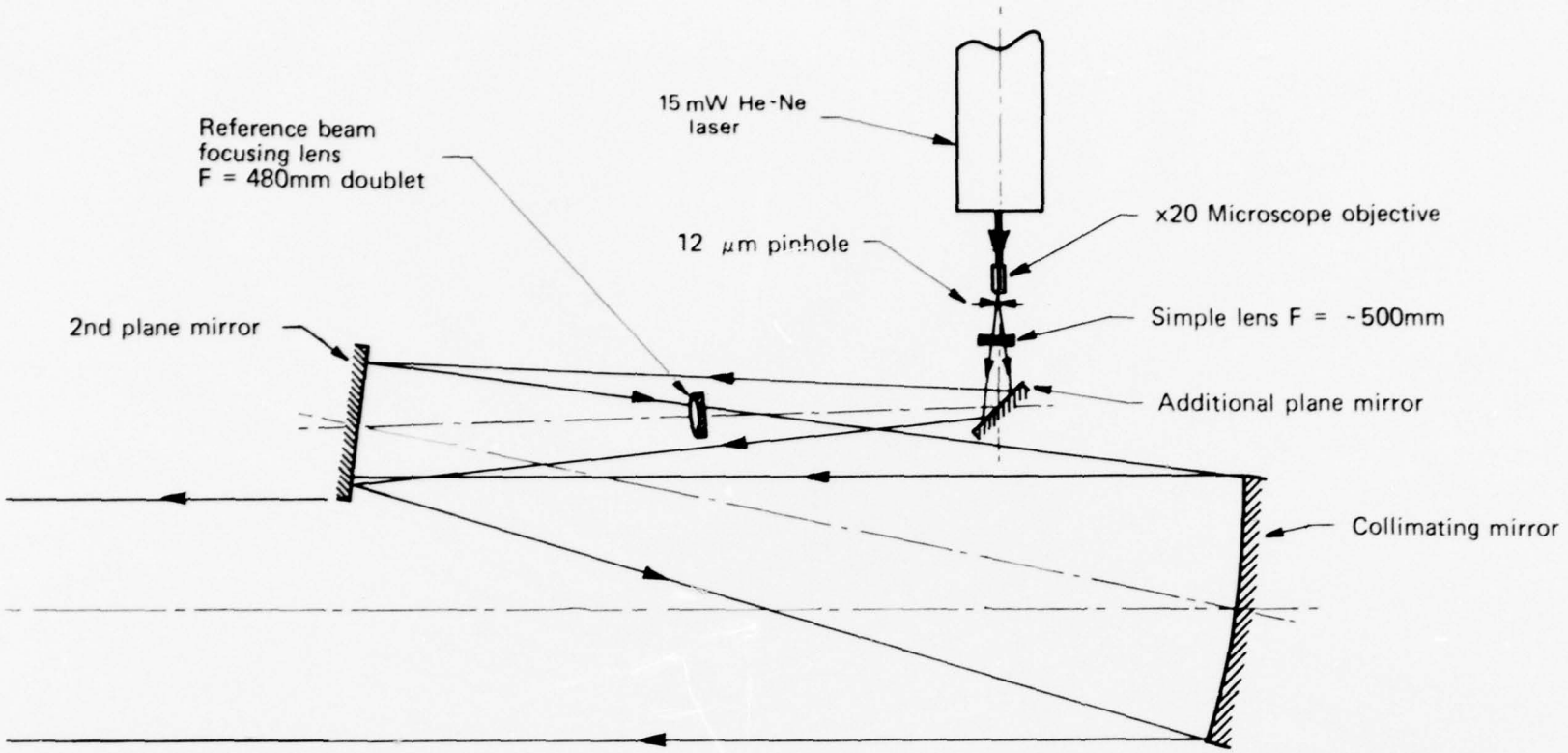

Note: For clarity ref. beam not shown

FIG. 8 DETAILS OF SOURCE END OF PROTOTYPE INTERFEROMETER

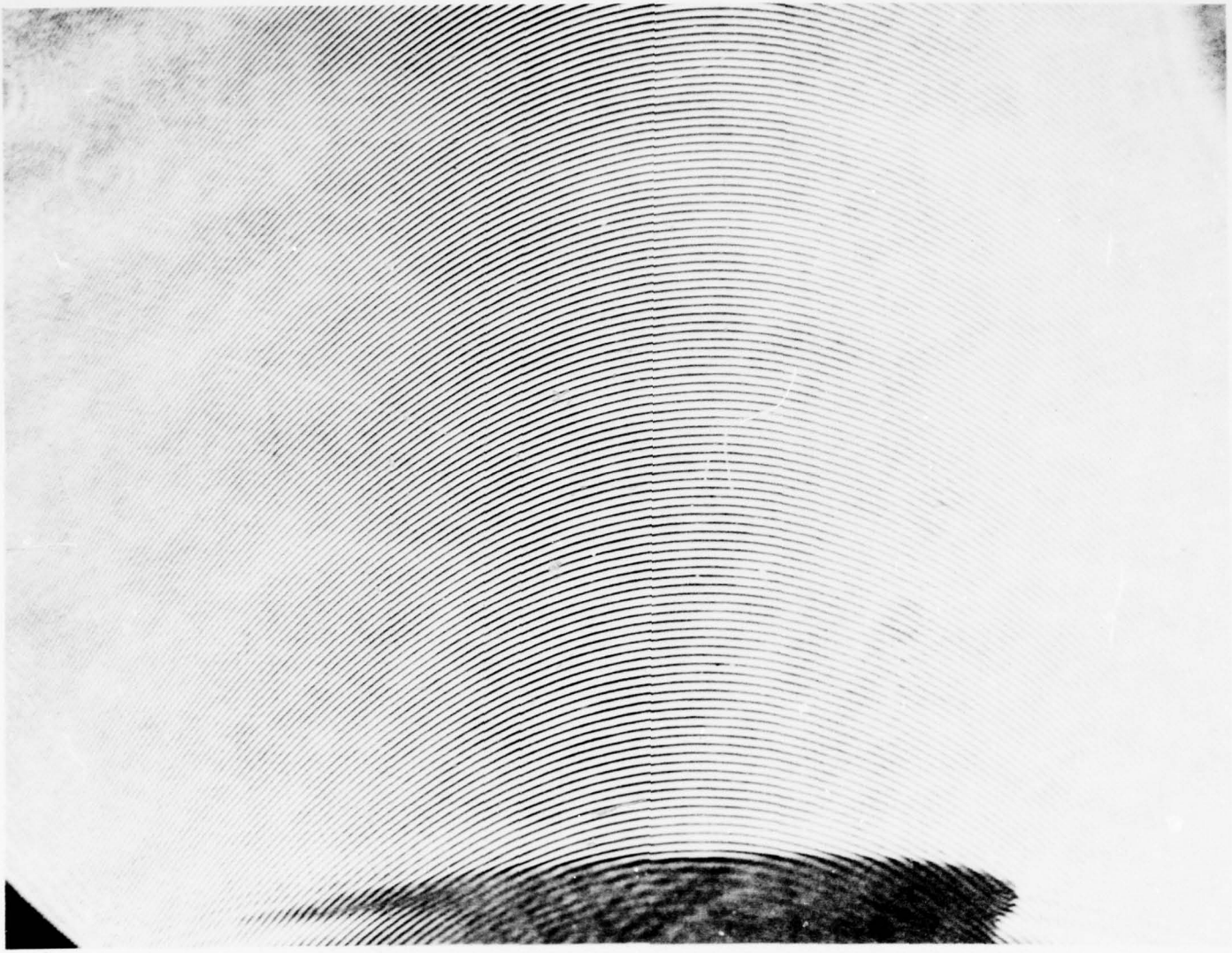

FIG. 9 NO FLOW INTERFEROGRAM (Coarse fringe spacing)

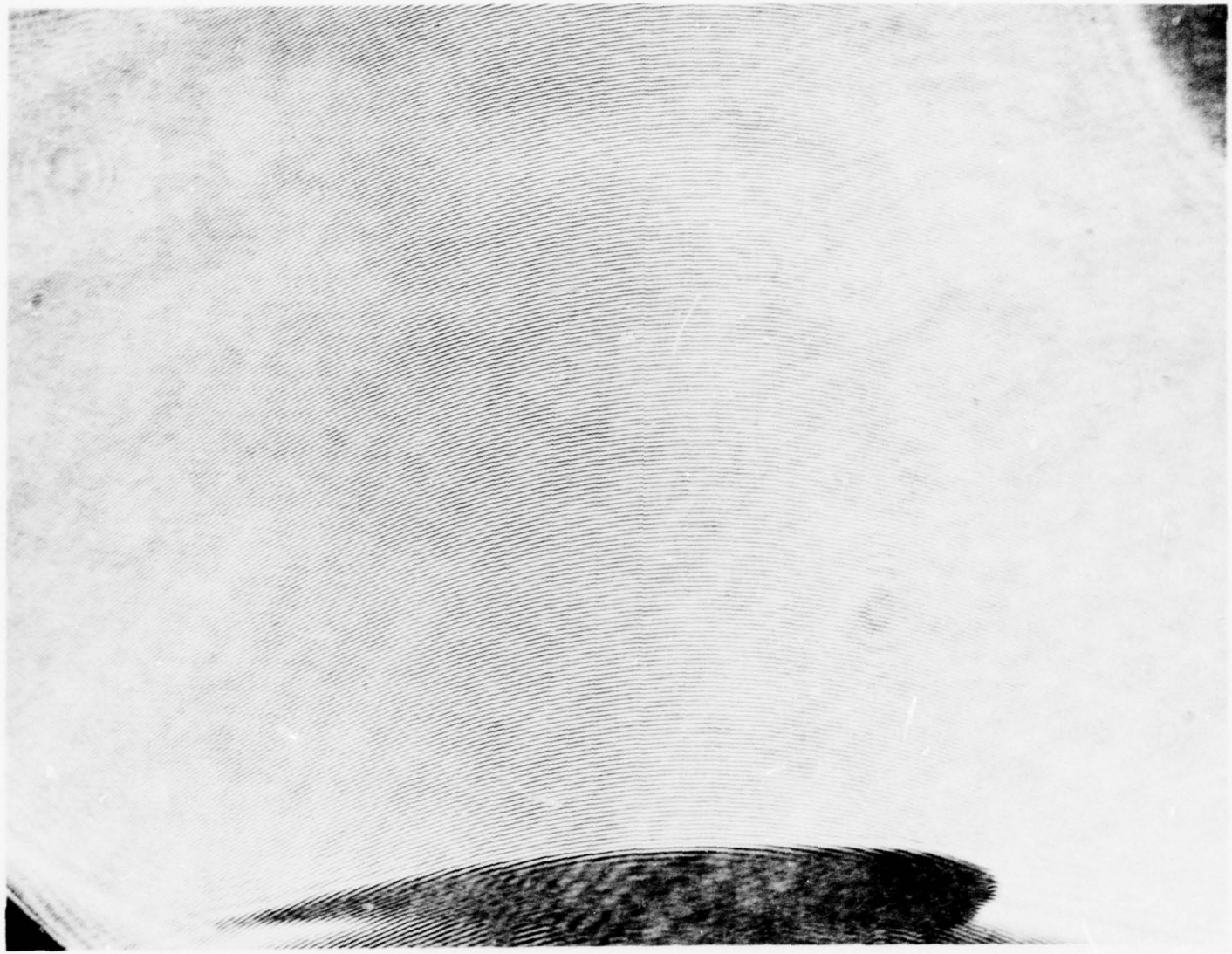

FIG. 10 NO FLOW INTERFEROGRAM (Medium fringe spacing)

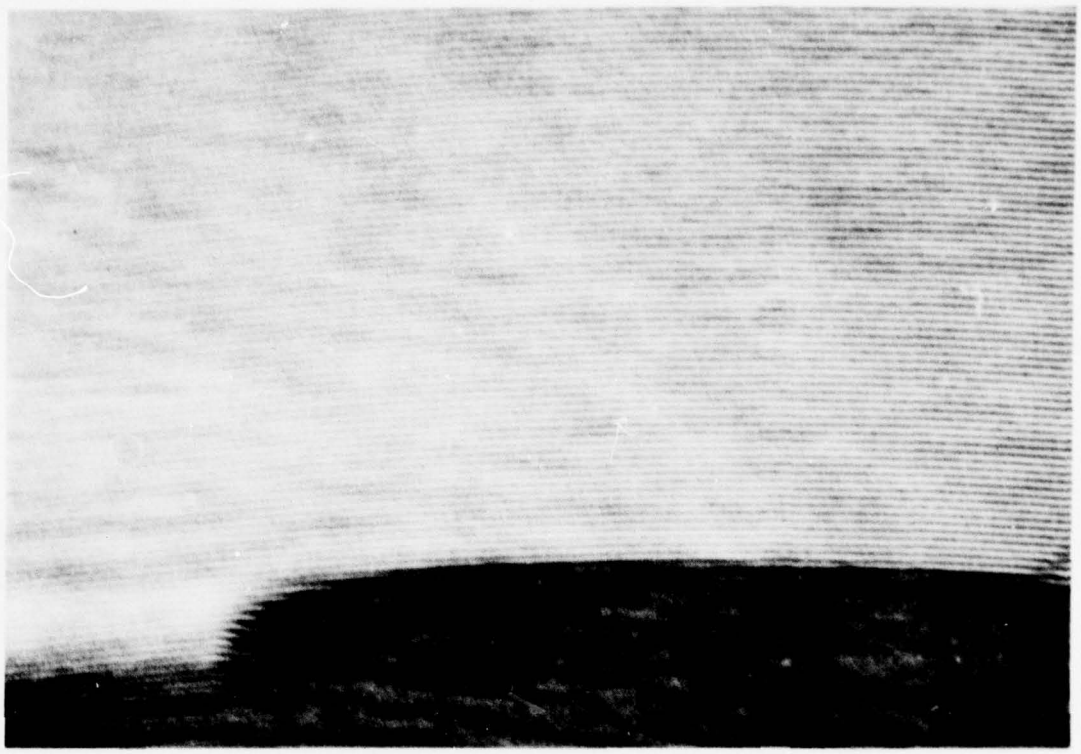

No flow

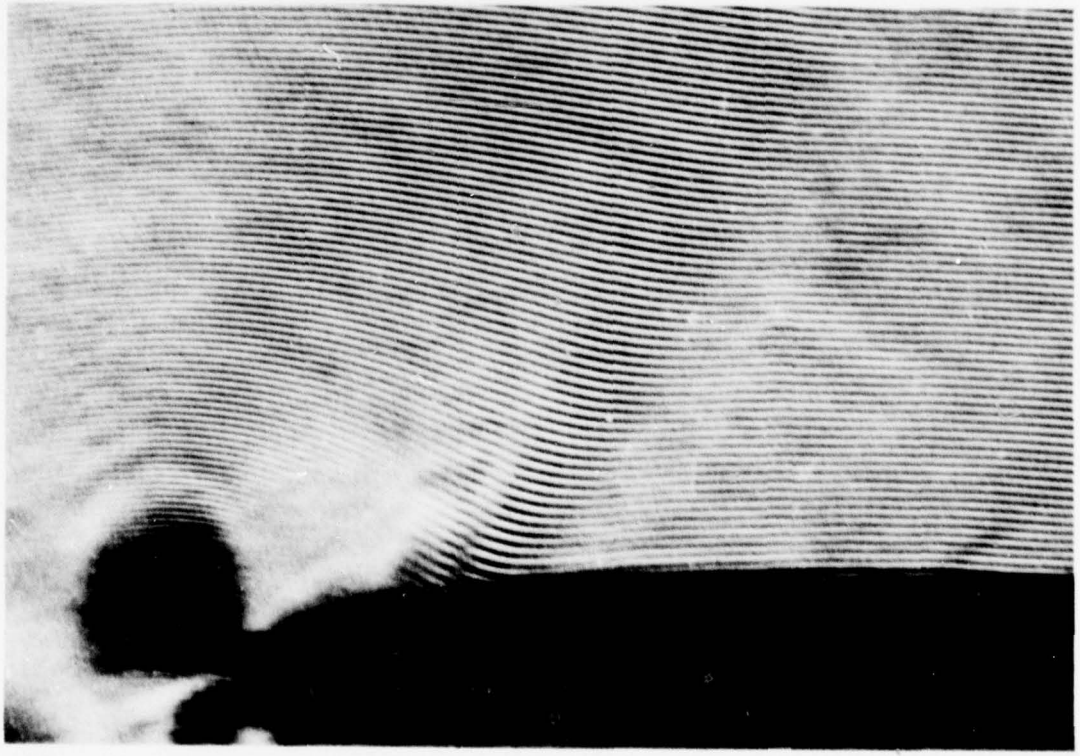

With flow

FIG. 11 FINE FRINGE INTERFEROGRAMS
(Area near aerofoil leading edge)

Typical pair of interferograms in optimum alignment

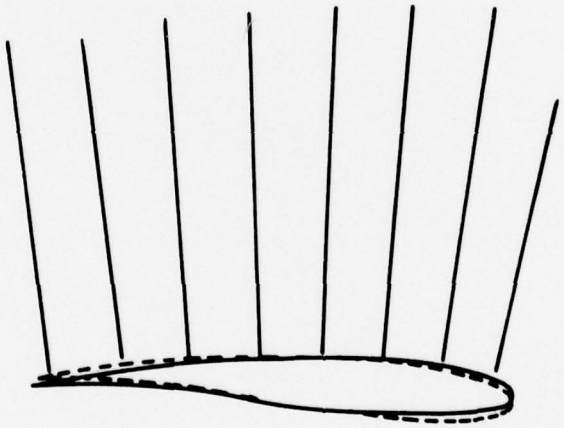

Identical interferograms with 1° angular rotation

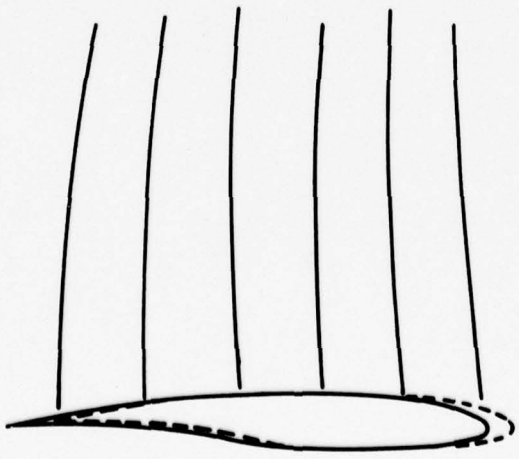

Identical interferograms with 5%C chordwise translation

FIG. 12 FRINGES FORMED BY SUPERPOSITION OF TWO NO FLOW INTERFEROGRAMS

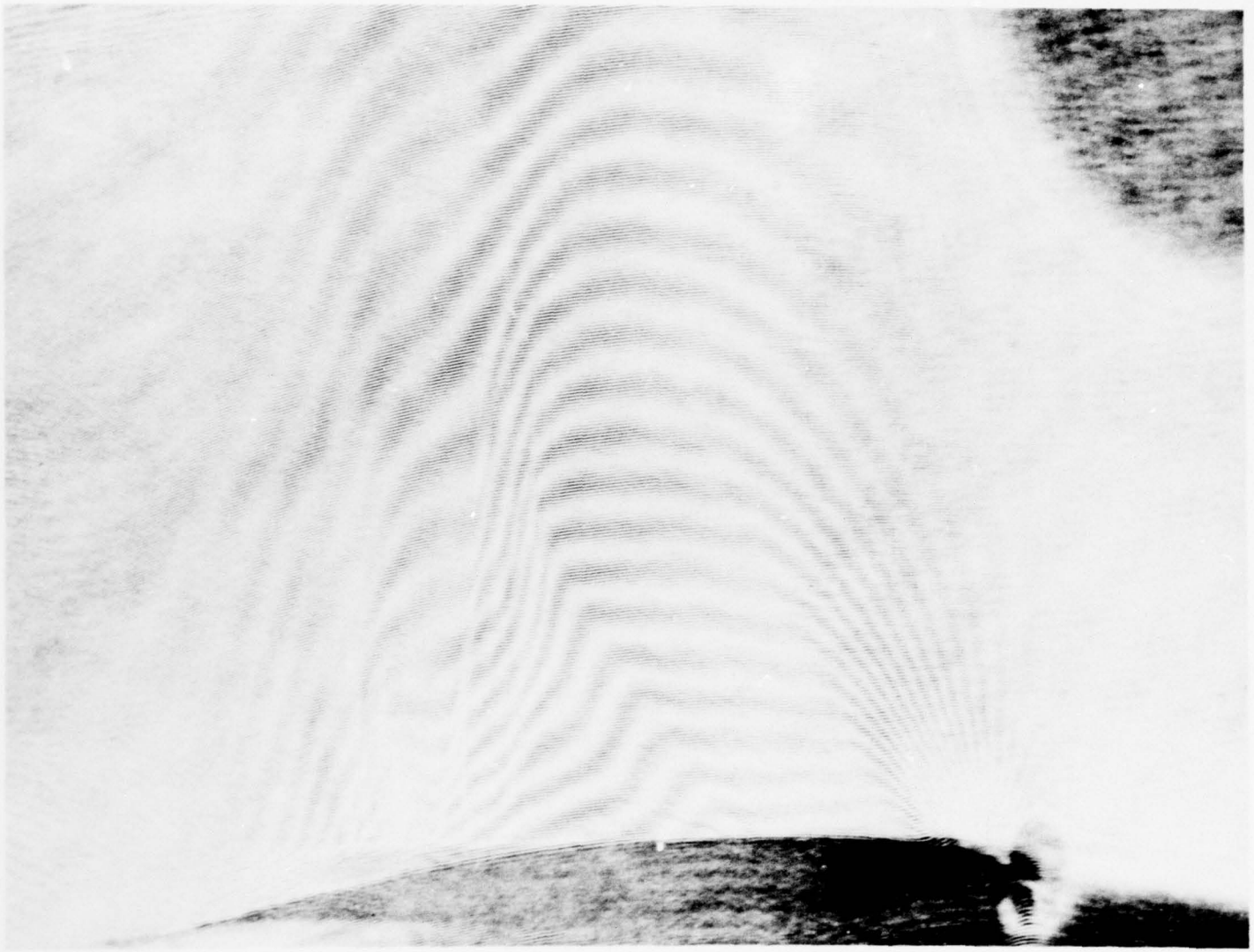

FIG. 13 COMPOSITE INTERFEROGRAM OF UPPER SURFACE FLOW ON SUPERCRITICAL AEROFOIL
BGK = 1 ($M = 0.80$, $\alpha = 1.4°$, $R = 1.2 \times 10^6$)

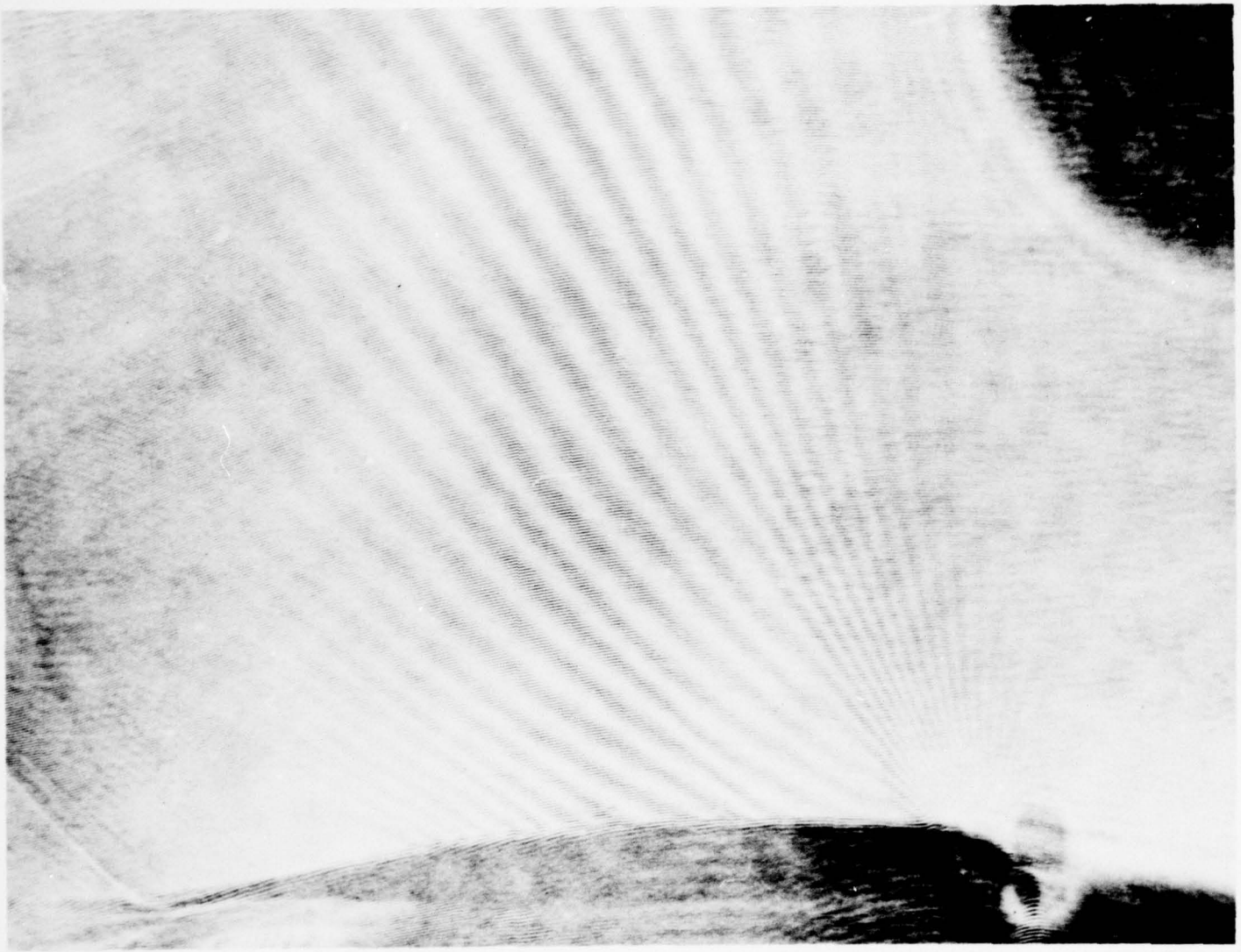

FIG. 14 COMPOSITE INTERFEROGRAM OF UPPER SURFACE FLOW ON SUPERCRITICAL AEROFOIL
BGK ≈ 1 ($M \triangleq 1.00$, $\alpha = 1.4°$, $R = 1.2 \times 10^6$)

M = 0.756

α = 1.4°

R = 1.6 x 10^6

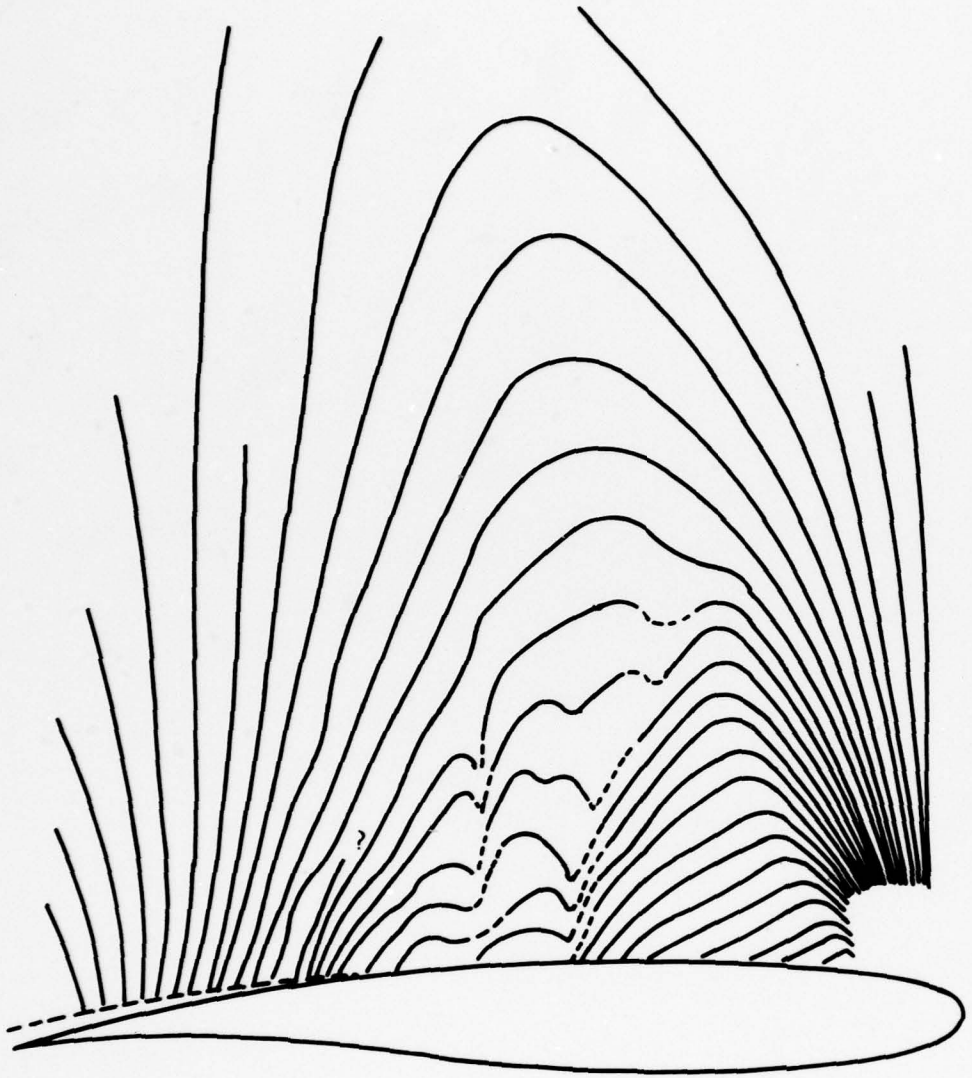

FIG. 15 INTERFEROGRAM – SUPERCRITICAL AEROFOIL BGK--1

M = 0.763

α = 1.4°

R = 1.6 x 10^6

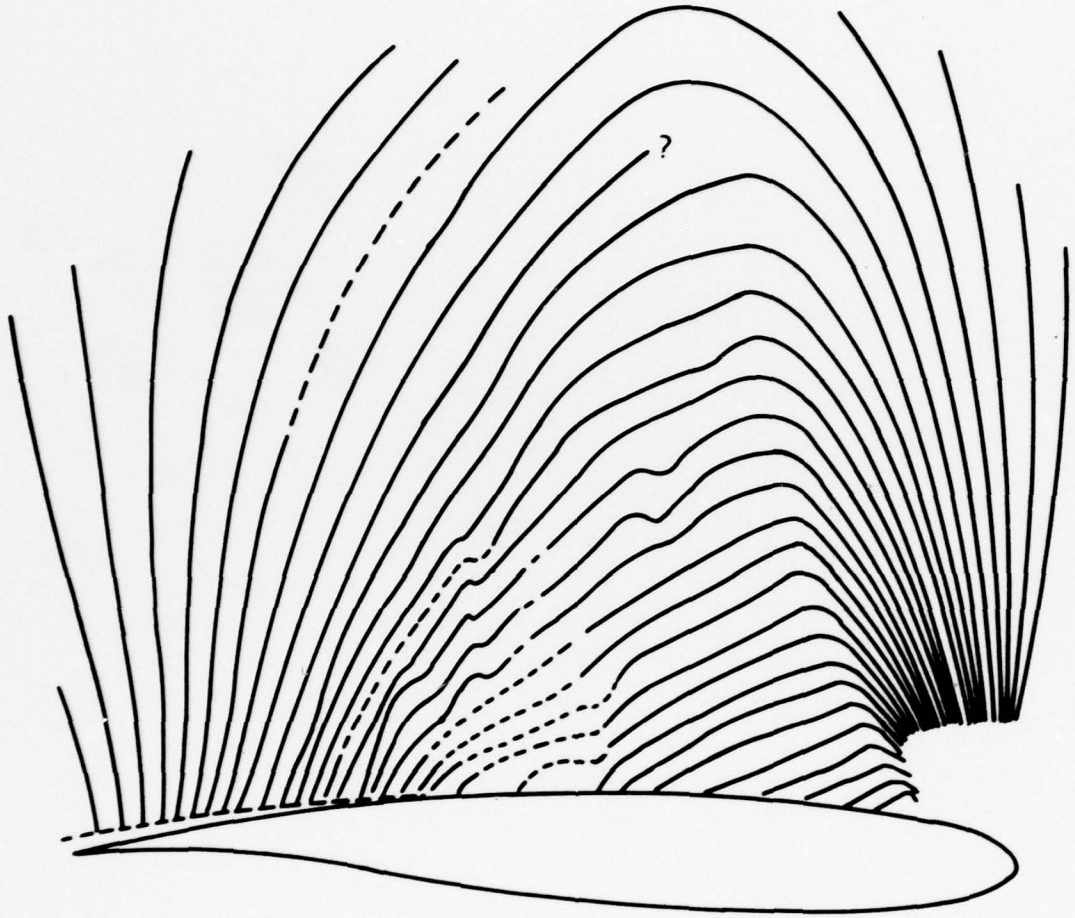

FIG. 16 INTERFEROGRAM – SUPERCRITICAL AEROFOIL BGK–1

M = 0.782

α = 1.4°

R = 1.6 x 10^6

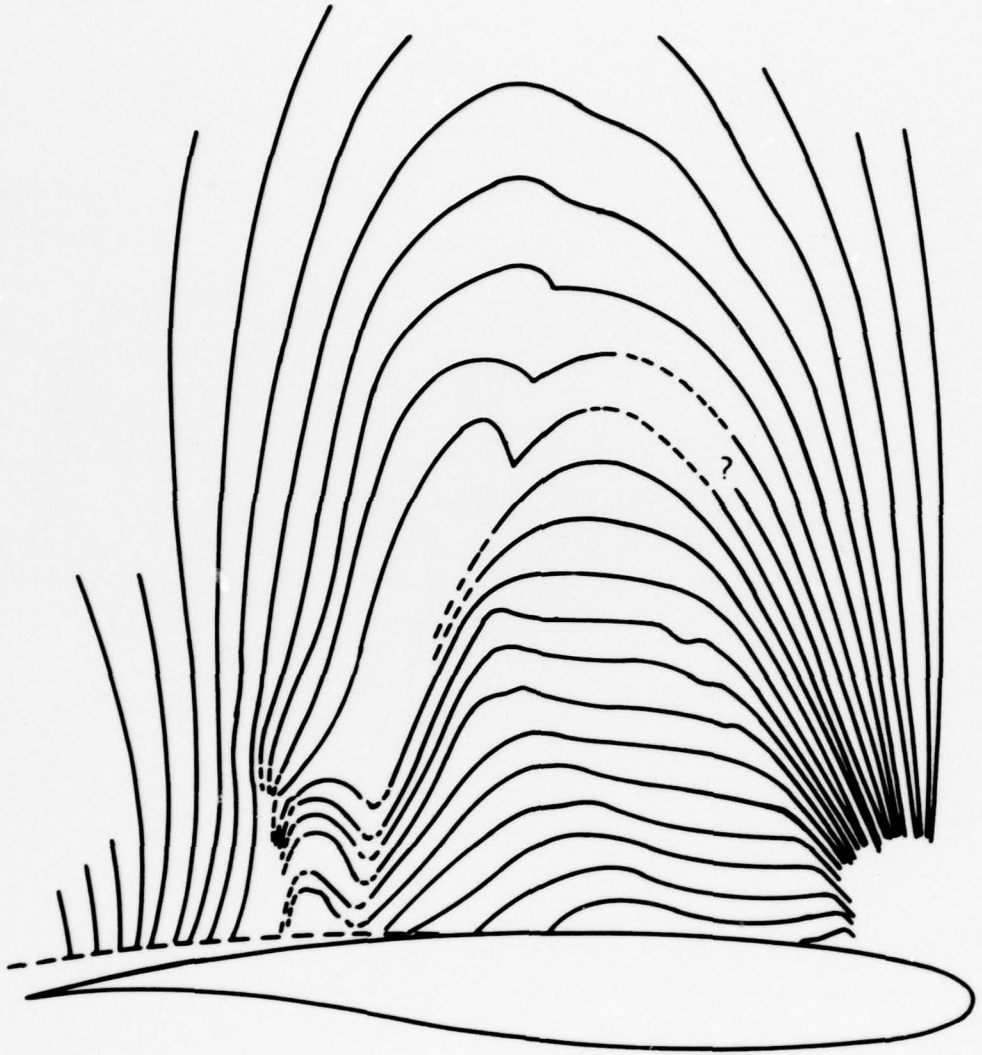

FIG. 17 INTERFEROGRAM – SUPERCRITICAL AEROFOIL BGK-1

M = 0.900

α = 1.4°

R = 1.2 x 10^6

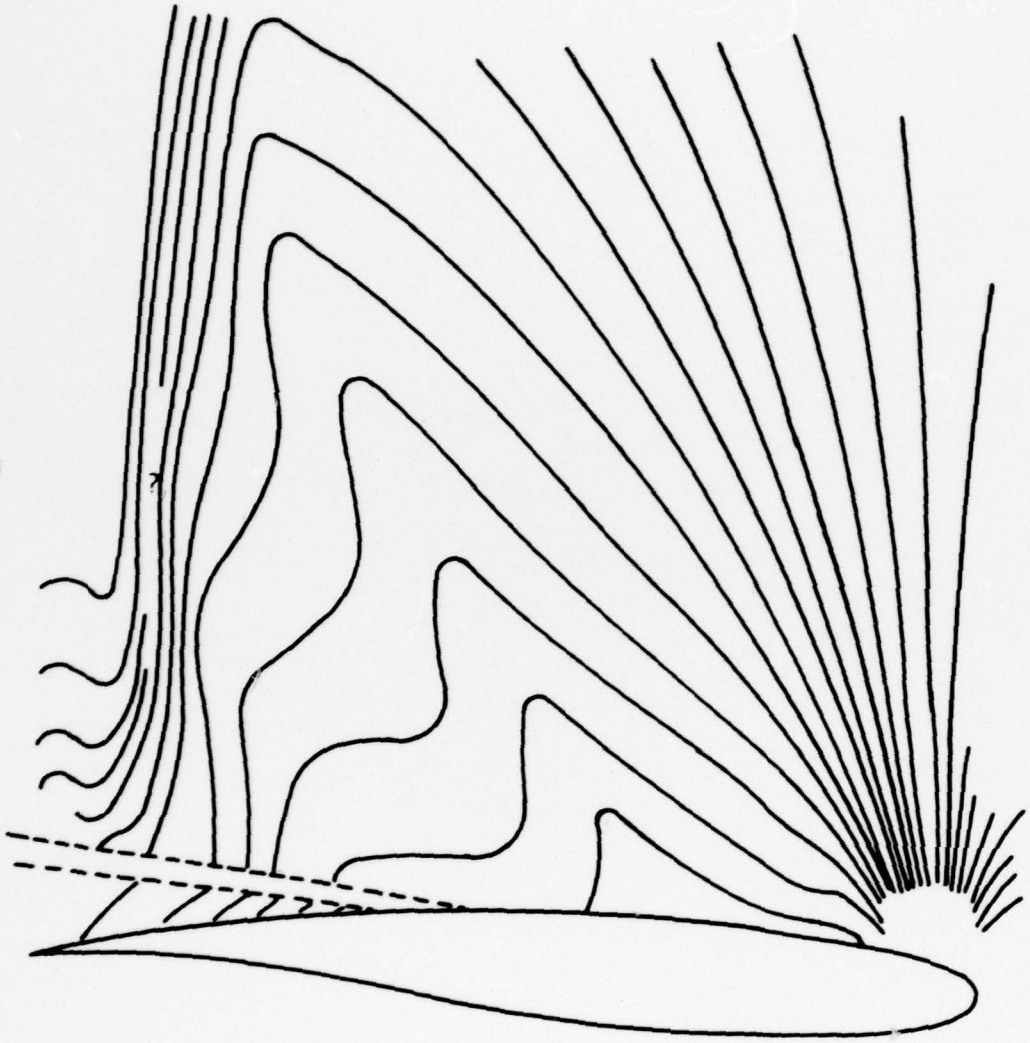

FIG. 18 INTERFEROGRAM -- SUPERCRITICAL AEROFOIL BGK--1

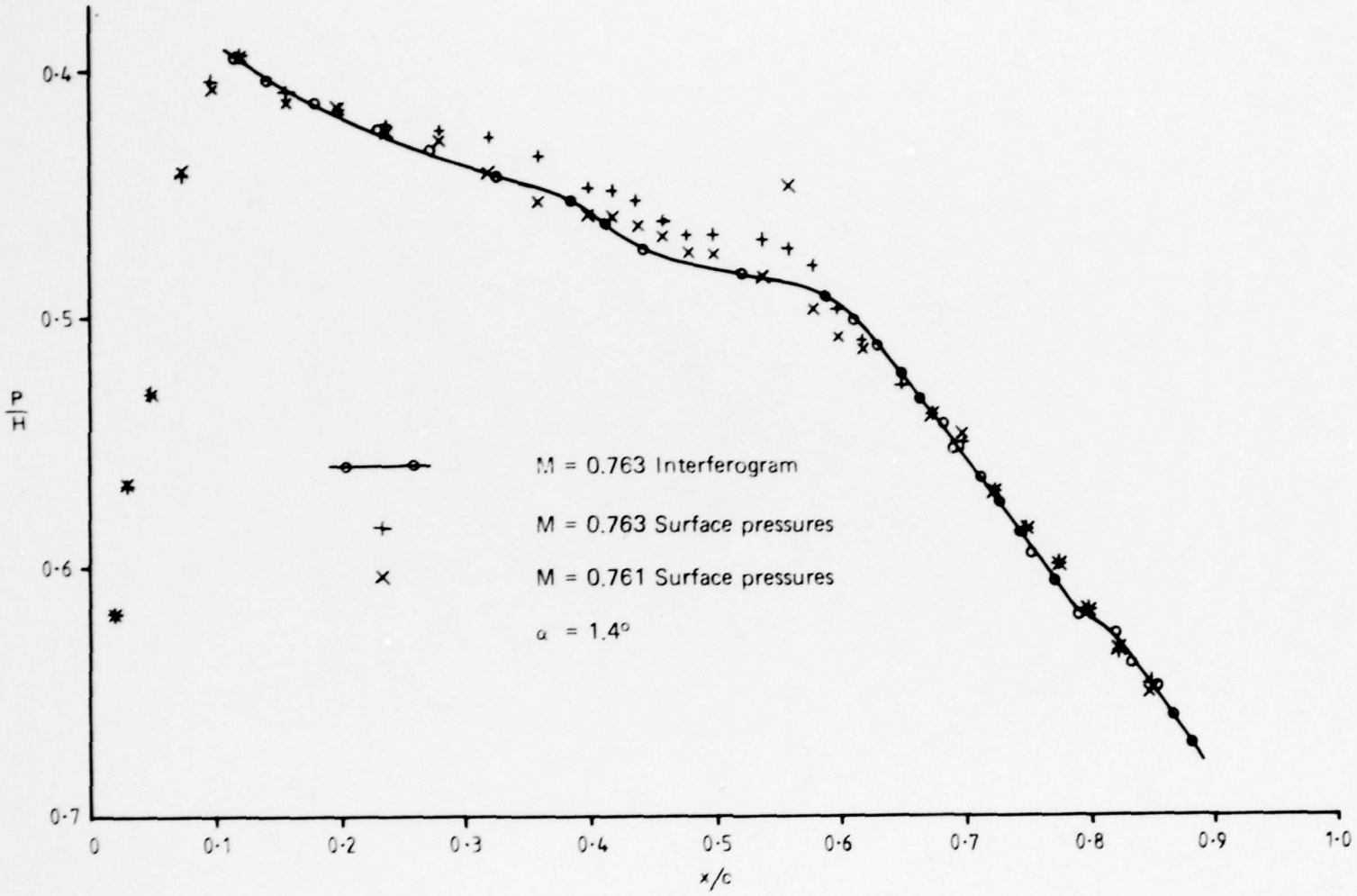

FIG. 19 PRESSURE DISTRIBUTION ON UPPER SURFACE OF SUPERCRITICAL AEROFOIL BGK–1

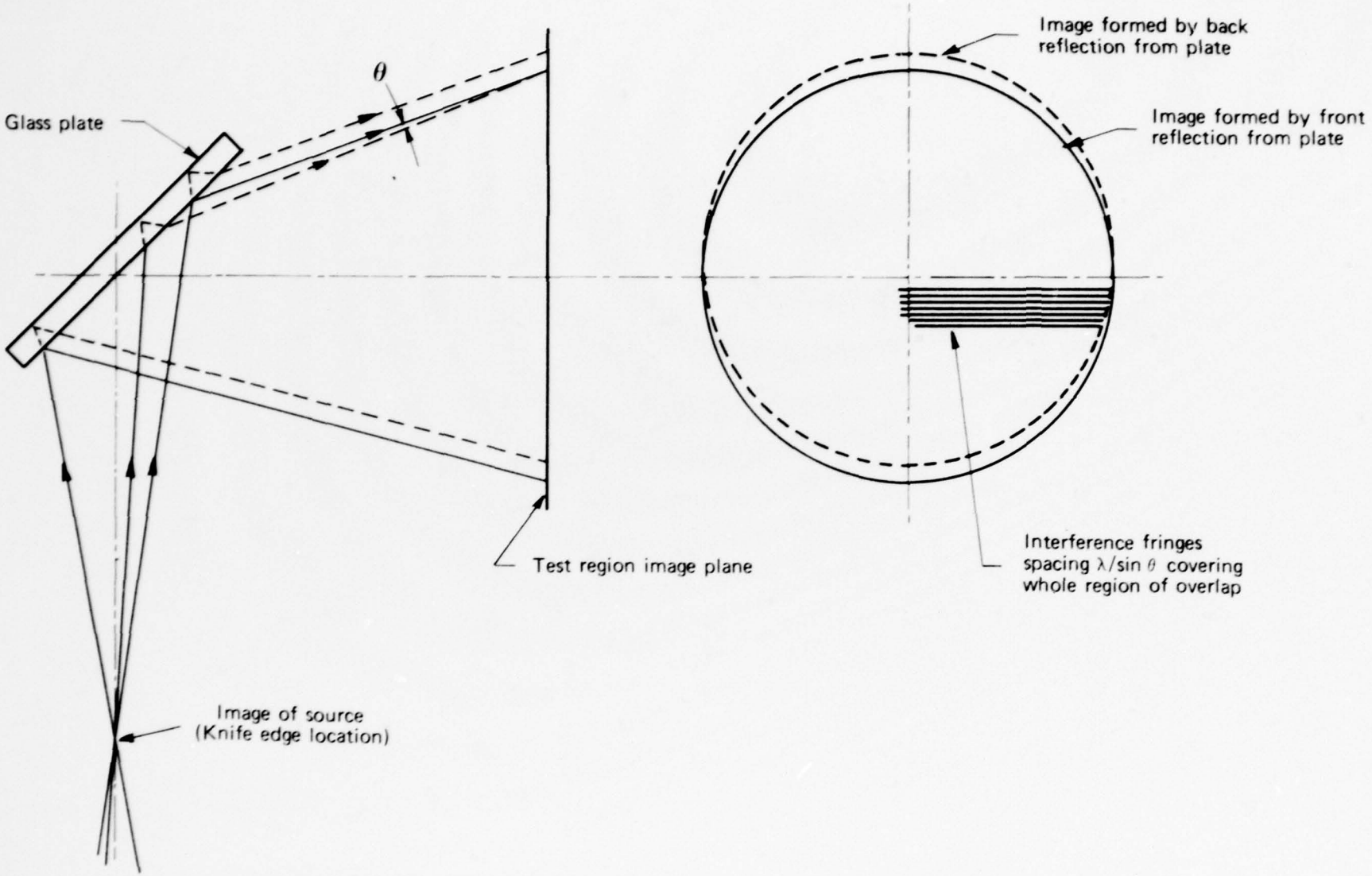

FIG. 20 ARRANGEMENT OF MURTY-TANNER INTERFEROMETER

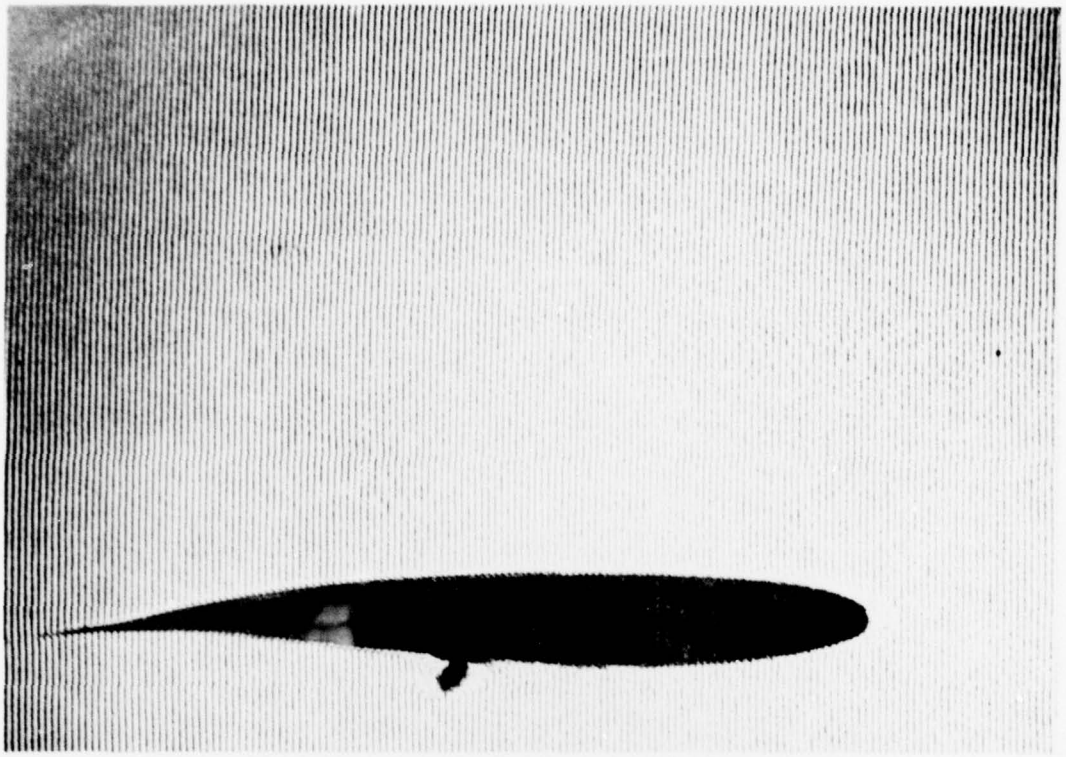

No. flow

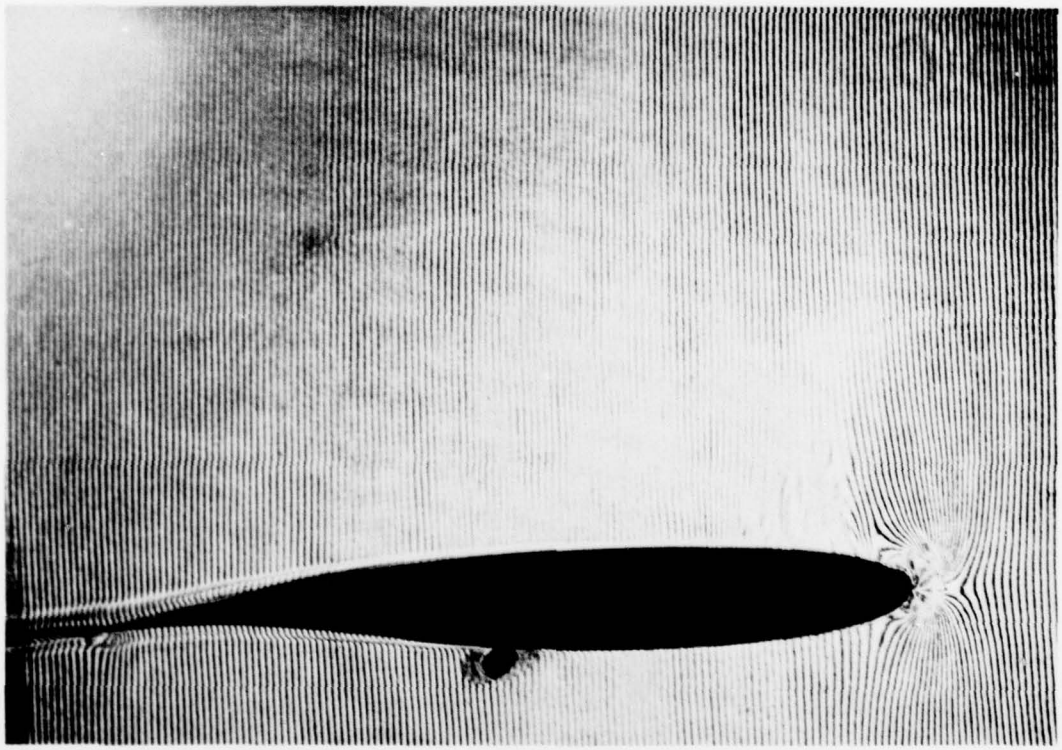

M ≃ 0.75

FIG. 21 INTERFEROGRAMS FROM BEAM SHEARING INTERFEROMETER
(Supercritical aerofoil BGK–1)

DOCUMENT CONTROL DATA SHEET

Security classification of this page: Unclassified

1. Document Numbers
   (a) AR Number:
   AR-001-281
   (b) Document Series and Number:
   Aerodynamics Note 378
   (c) Report Number:
   ARL-Aero-Note-378

2. Security Classification
   (a) Complete document:
   Unclassified
   (b) Title in isolation:
   Unclassified
   (c) Summary in isolation:
   Unclassified

3. Title: A SIMPLE METHOD OF ADAPTING A WIND TUNNEL SCHLIEREN SYSTEM FOR INTERFEROMETRY

4. Personal Author(s):
   N. Pollock

5. Document Date:
   June, 1978

6. Type of Report and Period Covered:

7. Corporate Author(s):
   Aeronautical Research Laboratories
   9. Cost Code: 54 7720

8. Reference Numbers
   (a) Task: DST 76/103
   (b) Sponsoring Agency:

10. Imprint:
    Aeronautical Research Laboratories,
    Melbourne

11. Computer Program(s)
    (Title(s) and Language(s)):

12. Release Limitations (of the document): Approved for public release

12-0. Overseas:	No.		P.R.	1	A		B		C		D		E	

13. Announcement Limitation (of the information on this page): No limitation

14. Descriptors:
    Flow Visualisation
    Lasers
    Interferometers
    Wind Tunnels
    Schlieren Photography

15. Cosati Codes: 1402
    1402

16.

ABSTRACT

A simple method of adapting a wind tunnel Schlieren system for interferometry is described. This new interferometer arrangement employs a laser light source, a lens which splits off the reference beam after test beam expansion and a lens and Lloyd mirror to recombine the two beams. The reference beam passes through the test section but is contracted to a narrow waist and displaced well away from the model location.

The proposed design combines a number of favourable characteristics which render it particularly useful for wind tunnel tests. These characteristics include: simplicity, optical robustness, low vibration sensitivity, modest coherence requirements and ease of interferogram analysis. The main disadvantage is that slightly less than half of the total field of view can be recorded on a single interferogram.

Interferograms obtained from tests on a prototype instrument based on a Schlieren system of low mechanical rigidity are presented. Also included is a comparison between aerofoil pressure distributions obtained by direct measurement and by interferogram analysis.

DISTRIBUTION

	Copy No.
AUSTRALIA	
DEPARTMENT OF DEFENCE	
Central Office	
Chief Defence Scientist	1
Executive Controller, ADSS	2
Superintendent, Defence Science Administration	3
Defence Library	4
Assistant Secretary, DISB	5–20
JIO	21
Australian Defence Scientific and Technical Representative (UK)	22
Counsellor, Defence Science (USA)	23
Aeronautical Research Laboratories	
Chief Superintendent	24
Superintendent, Aerodynamics	25
Divisional File, Aerodynamics	26
Author: N. Pollock	27
Library	28
Transonic Wind Tunnel Group	29–30
Materials Research Laboratories	
Library	31
Defence Research Centre	
Library	32
K. D. Thomson	33
Central Studies Establishment	
Library	34
Engineering Development Establishment	
Library	35
RAN Research Laboratory	
Library	36
Defence Regional Office	
Library	37
Navy Office	
Naval Scientific Adviser	38
Army Office	
Royal Military College, Library	39
Air Force Office	
Air Force Scientific Adviser	40
DEPARTMENT OF PRODUCTIVITY	
Government Aircraft Factories (Library)	41

STATUTORY AND STATE AUTHORITIES AND INDUSTRY

Australian Atomic Energy Commission (Director)		42
CSIRO Central Library		43
CSIRO Mechanical Engineering Division (Chief)		44
Gas and Fuel Corporation of Victoria		45
SEC Herman Research Laboratory (Librarian) Vic.		46
SEC of Queensland (Library)		47
Commonwealth Aircraft Corporation (Manager)		48

UNIVERSITIES AND COLLEGES

Adelaide	Barr Smith Library	49
Australian National	Library	50
Flinders	Library	51
James Cook	Library	52
Latrobe	Library	53
Melbourne	Engineering Library	54
	Professor Whitten, Mechanical Engineering	55
Monash	Library	56
Newcastle	Library	57
New England	Library	58
New South Wales	Physical Sciences Library	59
	Professor R. A. A. Bryant, Mech. & Ind. Eng.	60
	Professor A. H. Wills, Mech. & Ind. Eng.	61
Sydney	Professor G. A. Bird, Aero. Eng.	62
	Professor J. W. Roderick, Mech. Eng.	63
	Professor R. I. Tanner, Mech. Eng.	64
Queensland	Library	65
Tasmania	Engineering Library	66
	Professor A. R. Oliver, Civil & Mech. Eng.	67
Western Australia	Library	68
NSW Institute of Technology	Dr. S. L. Hall, Mech. Eng. Dept.	69
RMIT	Library	70

CANADA

NRC, National Aeronautical Est. Library	71
Energy, Mines and Resources Dept., Canadian Combustion Res. Labs., (Mr. B. Mitchell, Manager)	72
Gas Dynamics Laboratory, Mr. R.A. Tyler	73

UNIVERSITIES AND COLLEGES

McGill	Library	74
Toronto	Institute of Aerophysics	75

FRANCE

ONERA, Library	76
AGARD, Library	77
Service de Documentation, Technique de l'Aeronautique	78

GERMANY

ZLDI	79

INDIA

Defence Ministry, Aero. Development Establishment, Library	80
Hindustan Aeronautics Ltd., Library	81
Indian Institute of Science, Library	82
Indian Institute of Technology, Library	83
National Aeronautical Laboratory, Director	84

Cranfield Institute of	Library	124
Technology	Professor LeFebvre	125
Imperial College	The Head	126
	Professor B. G. Neal, Struc. Eng.	127
	Professor, Mechanical Eng.	128
	P. Bradshaw, Dept. of Aeronautics	129

UNITED STATES OF AMERICA

NASA Scientific & Technical Information Facility		130
Sandia Group Research Organisation		131
American Institute of Aeronautics and Astronautics		132
The John Crerar Library		133
Allis Chalmers Inc., Library		134
Applied Mechanics Reviews		135
United Technologies Corporation, *Fluid Dynamics Laboratories*		136
Battelle Memorial Institute, Library		137

UNIVERSITIES AND COLLEGES

Cornell (New York)	Library, Aeronautical Laboratories	138
Harvard	Professor A. F. Carrier, Div. of Eng. and Applied Maths.	139
	Dr. S. Goldstein	140
	Professor H. M. Emmons	141
Iowa State	Dr. G. K. Serory, Mech. Eng.	142
George Washington	Professor Freudenthal	143
Brooklyn	Library, Poltech. Aero. Lab.	144
California	Library, Guggenheim Aero. Lab.	145
	Dr. M. Holt, Dept. of Aero. Sciences	146
Florida	Mark H. Clarkson, Dept. of Aero. Eng.	147
Johns Hopkins	Professor S. Corrsin, Dept. of Mech. Eng.	148
Illinois	Professor N. M. Newmark, Talbot Laboratories	149
Stanford	Library, Dept. of Aeronautics	150
Wisconsin	Memorial Library, Serials Department	151
MIT	Professor E. Ressner	152
Spares		153–162